SUPERRESOLUTION USING INCOHERENT LIGHT AND THE LEAST SQUARES METHOD

THESIS

Robert F. Stierwalt
Captain, USAF

AFIT/GEO/ENP/85D-5

DEPARTMENT OF THE AIR FORCE
AIR UNIVERSITY
AIR FORCE INSTITUTE OF TECHNOLOGY

Wright-Patterson Air Force Base, Ohio

AFIT/GEO/ENP/85

DTIC
ELECTE
FEB 1 3 1986
S D
D

SUPERRESOLUTION USING INCOHERENT LIGHT

AND THE LEAST SQUARES METHOD

THESIS

Robert F. Stierwalt
Captain, USAF

AFIT/GEO/ENP/85D-5

AFIT/GEO/ENP/85D-5

SUPERRESOLUTION USING INCOHERENT LIGHT AND THE LEAST SQUARES METHOD

THESIS

Presented to the Faculty of the School of Engineering

of the Air Force Institute of Technology

Air University

In partial Fulfillment of the

Requirements for the Degree of

Master of Science in Electrical Engineering

Accesion For	
NTIS CRA&I	☒
DTIC TAB	☐
Unannounced	☐
Justification	
By	
Distribution /	
Availability Codes	
Dist	Avail and / or Special
A-1	

Robert F. Stierwalt, B.S.,B.S.E.E.

Captain, USAF

December 1985

Approved for public release; distribution unlimited

Preface

This thesis represents the largest single undertaking I have ever attempted. The purpose of this thesis was to develop a superresolution method for resolving two incoherent point sources of light. This thesis was sponsored by the Air Force Armament Test Laboratory (AFATL) at Eglin AFB, FL.

I owe a debt of gratitude to the many people who would listen to my problems and help me stay on course. Specific thanks go to Capt Glenn Prescott from the Electrical Engineering Department and to Professor Jones from the Math department. These people were instrumental in their help in the overall thesis effort.

An even deeper appreciation goes to my thesis advisor, Major J.P. Mills whom I have learned to respect and admire for his technical and military expertise. Major Mills helped keep everything in perspective to allow me to keep working with a good attitude.

It goes without saying that every married person that goes to AFIT puts their spouse through a great deal of heartache and pain. My wife has endured two complete AFIT tours of 18 months each and deserves to be congratulated for being an "AFIT Widow" twice and still staying married to me.

Robert F. Stierwalt

Table of Contents

List of Figures

AFIT/GEO/ENP/85D-5

Abstract

This thesis discusses the problem of incoherent imaging in a diffraction limited optical system. The purpose of the thesis was to prove that resolving two incoherent point sources of light is possible and achievable under certain circumstances. The effects of noise are considered when trying to superresolve the two incoherent objects.

The analysis assumes a finite object of known maximum extent with an estimation of the noise in the system. The noise is assumed to be Gaussian, white, and additive for all spatial frequencies. The superresolution process uses the standard least squares process to achieve minimum error with a smoothing or regularization procedure. The singular values of the transfer matrix are modified to attenuate the very small singular values to avoid noise amplification in the high order terms. The effect of the noise is overcome by the use of a smoothing parameter, α, as shown in the results. The superresolution process works extremely well when the extent of the object is known a priori to have a certain bound or maximum. Components of the restored or processed object outside the known bounds are attenuated. The results indicate that band-pass pupils can superresolve with only limited knowledge of the object when the smoothing parameter is used.

SUPERRESOLUTION USING INCOHERENT LIGHT AND THE LEAST SQUARES METHOD

I. Introduction

The purpose of this thesis is to demonstrate that superresolution of two incoherent point sources is possible under certain conditions. Superresolution or resolving objects beyond classical limits is a current problem in optics. It is generally thought that diffraction effects represent the fundamental limits to optical system performance. Typically, objects placed closer than the classical Rayleigh limit (5:309) cannot be distinguished as distinct objects but image as a composite form. The physical dimensions of lens systems traditionally determine the ultimate resolving power of the system.

In many scientific disciplines (2:496) such as spectroscopy and astronomy, superresolution could enhance research considerably. In general, for a finite object in a diffraction limited imaging system, the inverse of the linear imaging process can be used to yield the object. In one specific example, an object of finite extent with known maximum dimensions can be superresolved to 20% of the traditional Rayleigh criterion for two incoherent point sources in a noise free system (3). However, in all cases the imaging process is noisy to some degree and usually produces a set of ill-conditioned linear equations, thus making the inversion of the imaging process suspect (4:216). Initially, the background and nature of incoherent imaging will be presented using a linear systems approach. Following the discussion of incoherent imaging, a specific plan for modeling a particular superresolution scheme will be presented as a research effort in order to determine if superresolution is practical and achievable under normal laboratory conditions.

Theory

Classically speaking, the normal limit to resolution for diffraction limited images is the Rayleigh criterion. Incoherent point sources image as a sinc squared function, $\mathrm{sinc}(x) = (\sin \pi x)/(\pi x)$, in a one dimensional system (1:62). Figure 1 illustrates the 1-D image for an object consisting

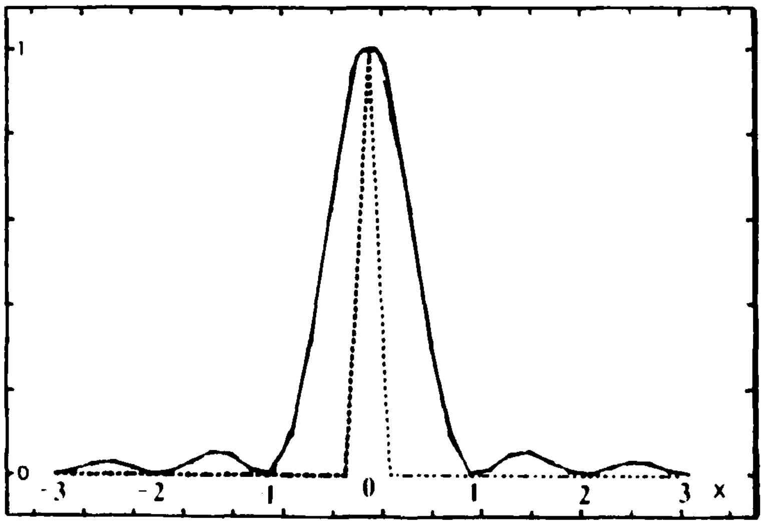

Figure 1. Impulse Response

of an incoherent point source. The image in this case is known as the impulse response of the imaging system. The dashed line represents the object and the solid line represents the diffraction limited image. Also, for incoherent light, the effect is additive in the irradiance distribution (amplitude squared) for two or more point sources.

For two adjacent, incoherent point sources, separated by the Rayleigh criteria, the irradiance distribution will be as shown in Figure 2. The solid line represents the total irradiance distribution while the dashed lines represent the individual irradiance distributions. Rayleigh defined the limit of resolution for circular apertures as the location of the first principle minimum of one irradiance distribution and the first principle maximum of the other irradiance distribution at the same point in the image plane. The same limit can be applied to rectangular apertures. In Figure 2, the irradiance has been normalized for clarity.

In 1964 J.L. Harris (3) used the concept of analytical continuation and a prior (known in advance) information about the object to extend resolution beyond the Rayleigh limit (5:309). Harris proved that continueing or extrapolating the function beyond the known bounds was possible using the fact that analytic functions are unique beyond the cutoff frequency of the filter used. He proved that sampling the irradiance distribution from a finite object of known extent could be used along with the properties of analytic functions

(1:133) to resolve two point sources separated by 20% of the classical Rayleigh resolution limit. This method of Harris used spectral extrapolation to reconstruct the object. Since the two point sources were

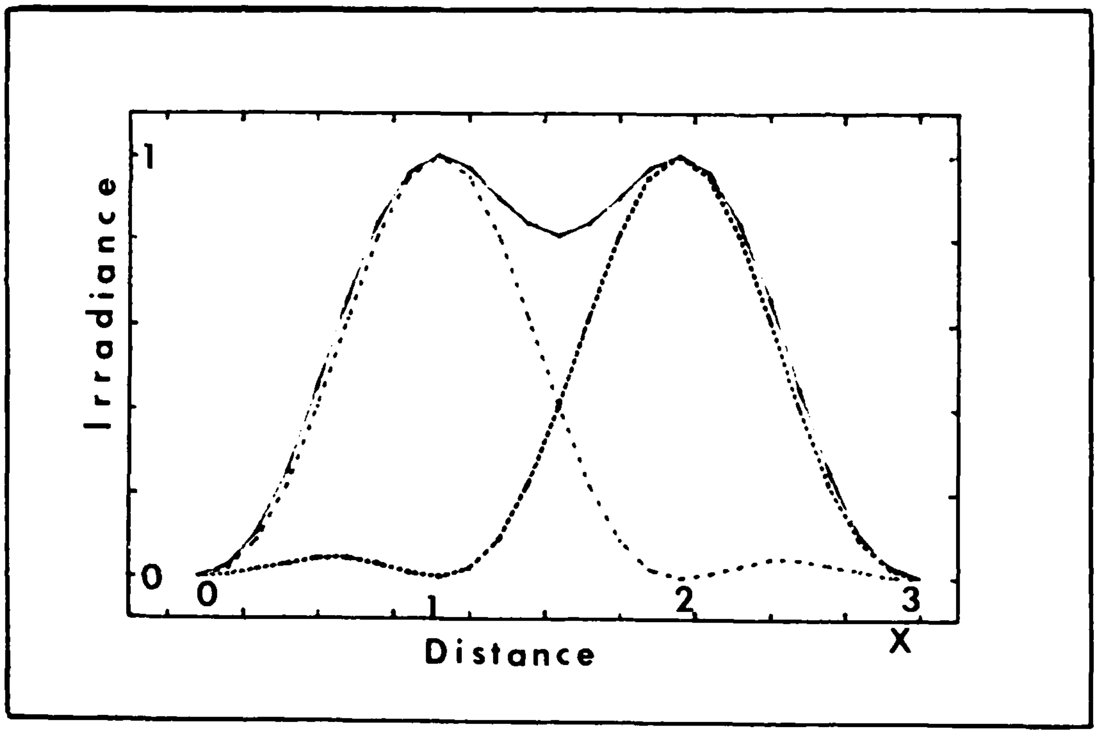

Figure 2. Minimum Rayleigh Resolution

closer than the Rayleigh criteria, this reconstruction scheme was also a superresolution process. This theory did not hold up under severe scrutiny as Harris neglected noise and did not know at the time that his set of simultaneous equations was extremely ill-conditioned (3:1481).

After analytical continuation was used to extrapolate the spectral components of a finite object with a priori knowledge of its maximum dimensions, it was realized that noise must be taken into account (6,7) to achieve any measurable degree of superresolution. One of the earliest methods used to superresolve objects was the iteration method proposed by Gerchberg (7). Gerchberg utilized a specific iteration method derived from the general method of Youla (8). The method of Youla uses orthogonal projections in a well-posed Hilbert space and a priori knowledge of the extent of the object to remove any spectral component higher than the cut-off frequency. Gerchberg theorized that any component measured at a higher frequency than the cut-off frequency had to be a noise component, and was therefore subtracted out. This method was iterated until the measured output past the cut-off frequency was below some threshold level. Gerchberg also reasoned that noise could not be analytically continued since it was not band limited.

Gerchberg did not realize at the time that his matrix methods were unstable as Byrne, et al, pointed out in their 1983 article (6). Broadband noise served to cause spurious oscillations in the data making the restoration scheme suspect. After a good noise estimation was used, Byrne, et al, were able to use a Gerchberg type algorithm to obtain a reasonable superresolved object.

To further the work of superresolution, Mammone and Eichman (2) used optimum linear programming techniques to smooth the data thus providing a stable, well-conditioned matrix solution to the image restoration problem. Their initial assumption was similiar to that of Harris (3) in that the image irradiance could be sampled and the object reconstructed from a set of linear equations. The matrix solution can be represented as

$$\vec{i} = \bar{A}\vec{o} \tag{1.1}$$

where $\vec{i}$ and $\vec{o}$ are n dimensional vectors representing the image irradiance and object irradiance respectively. $\bar{A}$ is an n by n transformation matrix obtained from the discretized solution of the object vector $\vec{o}$ from

$$i(xi) = |h(xi;xo)|^2 * o(xo) \tag{1.2}$$

The complete description of incoherent imaging is contained in the next chapter. Mammone and Eichman chose to make the transformation matrix, $\bar{A}$, stable by filtering methods. By filtering, high frequency noise is eliminated as well as making the inversion of the matrix $\bar{A}$ possible, thus yielding a solution for $\vec{o}$.

While all of the above methods use spectral extrapolation and symmetric low pass spectral filters, Cathey, et al, (9) have proposed a superresolution concept utilizing the same bandwidth as the extrapolation method, but using bandpass, or multi-aperture systems and interpolation instead of extrapolation to achieve superresolution. It is postulated that for each imaging situation, there exists a potential "best" aperture window to superresolve the object.

Using similiar reconstruction techniques in the frequency domain, the object was consistently better resolved using band pass techniques instead of low pass filtering.

Research Proposal

In this thesis effort, incoherent light will be used along with a multiple aperture system to develop a mathematical model for superresolving an object. By using incoherent light, the transfer function of the pupil, or aperture, is not as straight forward as the coherent case, but the matrix method of inverting the transformation matrix seems viable. To effectively evaluate the optimum pupil function, that pupil function yielding the minimum error will be judged as the best pupil function for a given fill ratio, where the fill ratio is the number of apertures divided by the total number of available windows (9:247). The premise to be proved is that for a given fill ratio, band pass filtering instead of low pass filtering provides better resolution using the proposed algorithm.

II. Theory of Incoherent Imaging

The purpose of this chapter is to summarize the theory of incoherent imaging. This summary utilizes a linear systems approach similiar to chapter six of reference one. By using a systems approach, the properties of an optical system can be given in terms of input, transfer function or impulse response, and output, irrespective of the number and type of internal optical elements. For optical systems, these properties can be summarized in terms of its exit or entrance pupil, effective focal length, and its output with an input consisting of a point source on the optic axis. In this particular case, images are located as predicted by geometric optics and the system is considered to be diffraction limited (1:103).

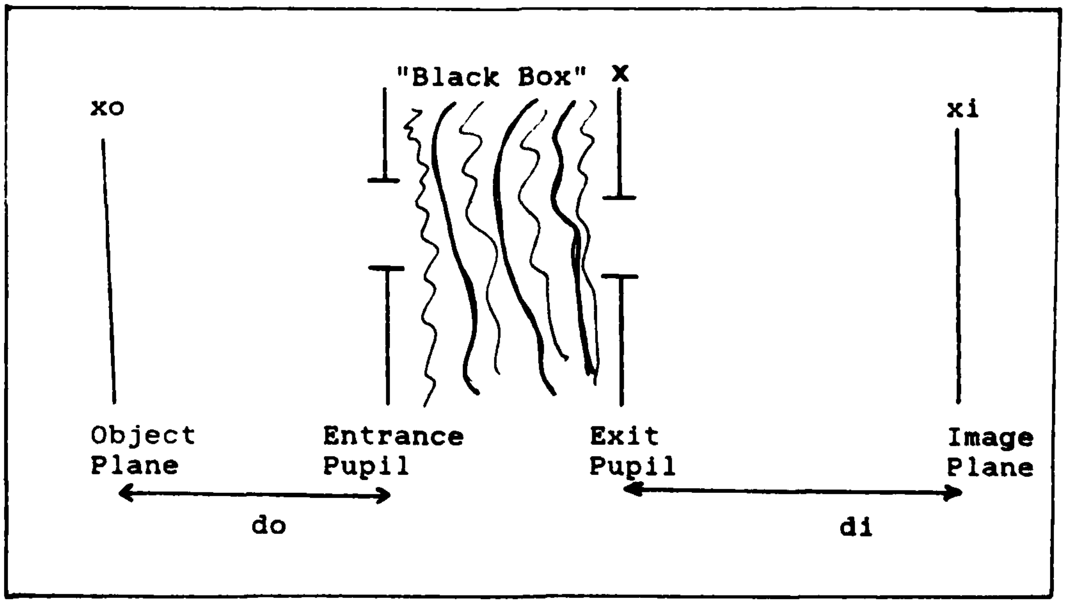

FIGURE 3. Generalized 1-D Image Model

Referring to figure 3, the imaging system can be represented as a "black box" consisting of an entrance pupil and an exit pupil. The properties of the entire system can be completely described by specifying the properties of the entrance pupil or exit pupil. It is assumed that the entire optical system can be adequately described by geometric optics and that all diffraction effects can be associated with the entrance or exit pupil. The entrance and exit pupils are geometric projections of one another which enables an equivalent analysis using either one (1:102-103).

Since geometric optics adequately describe the behavior of light between the entrance and exit pupils, diffraction dominates the behavior of light from the object to the entrance pupil and from the exit pupil to the geometric image plane. Since diffraction effects can be associated with either the entrance or exit pupil, all diffraction effects will be associated with the exit pupil in the context of this paper. This approach is acceptable since the exit and entrance pupil are geometric images of each other (1:102).

Using the notation found in Goodman's text (1) the image amplitude distribution can be expressed as

$$U_i(xi) = \int_{-\infty}^{\infty} h(xi;xo)U_o(xo)dxo \qquad (2.1)$$

where $U_i(xi)$ is the image amplitude, h(xi) is the impulse response or transfer function, and $U_o(xo)$ is the object amplitude distribution. The image plane is xi, the object plane xo, and the exit pupil plane is x. If the lens law for imaging is satisfied, then h(xi) is the Fraunhofer diffraction pattern of the exit pupil centered at xi = -Mxo , where M is the magnification of the system. Notice that the system is inverted as represented by the negative sign (1:95). The impulse response can be written as

$$h(xi;xo) = k\int_{-\infty}^{\infty} P(x)\exp\Big((-2\pi j/\lambda di)(xi-Mxo)x\Big)dx \qquad (2.2)$$

with the understanding that the pupil function, P(x), is either zero or one depending on whether it blocks or passes light in that particular interval, dx. In equation (2.2), h(xi;xo) can be described as the Fourier Transform (FT) of the pupil function evaluated at the spatial frequencies fx = $xi/\lambda di$. Also, K is a complex constant that will be discussed later. By appropiate change of variables, the impulse response can be rewritten as

$$h'(xi;xo) = k\int_{-\infty}^{\infty} P(\lambda dix')\exp\Big(-2\pi j(xi-xo')\Big)dx' \qquad (2.3)$$

where $x' = x/\lambda di$ and $xo' = Mxo$. By defining $U_g(xi)$ as the geometric image, the real image can be described as the convolution of the geometric image with h'(xi), the modified impulse response. Equation (2.4) is the convolution integral representing the final image as the convolution of the geometric image with the modified impulse response, h'(xi).

$$U_i(xi) = k\int_{-\infty}^{\infty} h'(xi-xo')U_g(xo')dxo' \qquad (2.4)$$

Since the final expression will be normalized with respect to magnitude, all constant multipliers, real or complex can be ignored (1:105).

Up to this point, amplitude has been the subject of our derivations, but irradiance (watts/area) is the measured quantity. The irradiance is the infinite time average of the amplitude squared as shown in equation (2.5).

$$I_i = \left\langle U_i(xi)U_i^*(xi)\right\rangle \qquad (2.5)$$

The brackets denote the infinite time average and $U_i^*(xi)$ designates the complex conjugate of $U_i(xi)$. For real sources and incoherent light,

$$I_g(xo) = \left\langle U_g(xo)\right\rangle^2 \qquad (2.6)$$

where g designates geometrically predicted quantities. The final irradiance image is

$$I_i(xi) = k\int_{-\infty}^{\infty} |h(xi-xo')|^2 I_g(xo')dxo' \qquad (2.7)$$

where the k represents a constant multiplier. It can be easily seen that the final irradiance image is again a convolution of a transfer function and a predicted geometric quantity. The irradiance transfer function is the modulus of the impulse response, h'(xi), squared. This implies that there is no phase information for incoherent imaging.(1:109)

For ease and convenience, let

$$G_g(fx) = \frac{FT(I_g(xo'))}{FT(I_g(xo'))}, \text{ evaluated at } fx=0 \qquad (2.8)$$

where $G_g(fx)$ represents the normalized Fourier transform of the geometrically predicted irradiance image of the object. Likewise

$$G_i(fx) = \frac{FT(I_i(xi))}{FT(I_i(xi))}, \text{ evaluated at } fx=0 \qquad (2.9)$$

where G (fx) is the normalized Fourier transform of the diffraction limited image. The irradiance transfer function, H(fx), is (1:114)

$$H(fx) = \frac{FT(|h'(xi)|^2)}{FT(|h'(xi)|^2)}, \text{ evaluated at } fx=0 \qquad (2.10)$$

where again normalization has taken place. Thus, in the frequency domain,

$$G_i(fx) = H(fx)G_g(fx) \qquad (2.11)$$

This last equation can be derived using the convolution theorem (13:314).

The optical transfer function, H, of the incoherent irradiance imaging system is

$$\mathbf{H} = |FT(h')|^2 \tag{2.12}$$

where

$$h' = FT(P) \tag{2.13}$$

It can be shown that for f(x) a real function of x that

$$FT(f(x) ** f(x)) = |FT(f(x))|^2 \tag{2.14}$$

By using the autocorrelation theorem (13:200). Therefore

$$|FT(h')|^2 = P**P \tag{2.15}$$

which leads to the final expression for the optical transfer function, H:

$$H = P**P \tag{2.16}$$

where ** denotes autocorrelation. Also, all subscripts, etc, have been dropped for clarity. Now, equation (2.11) can be expressed as

$$G_i = (P*P)G_g \tag{2.17}$$

which is the final spectral domain representation of the imaging relationship between the object and the optical system. Figure 4 illustrates the normalized transfer function for a rectangular pupil function. As can be seen, the OTF, H, has a definite cutoff frequency, fc, which is a function of the system parameters. The modulus of H, $|H|$, is known as the modulation transfer function, MTF (1:114).

For optical systems it would seem that a simple Fourier inverse of the frequency domain representation of the image would easily yield the original object. Equation (2.18) represents the inverse Fourier transform needed to recover

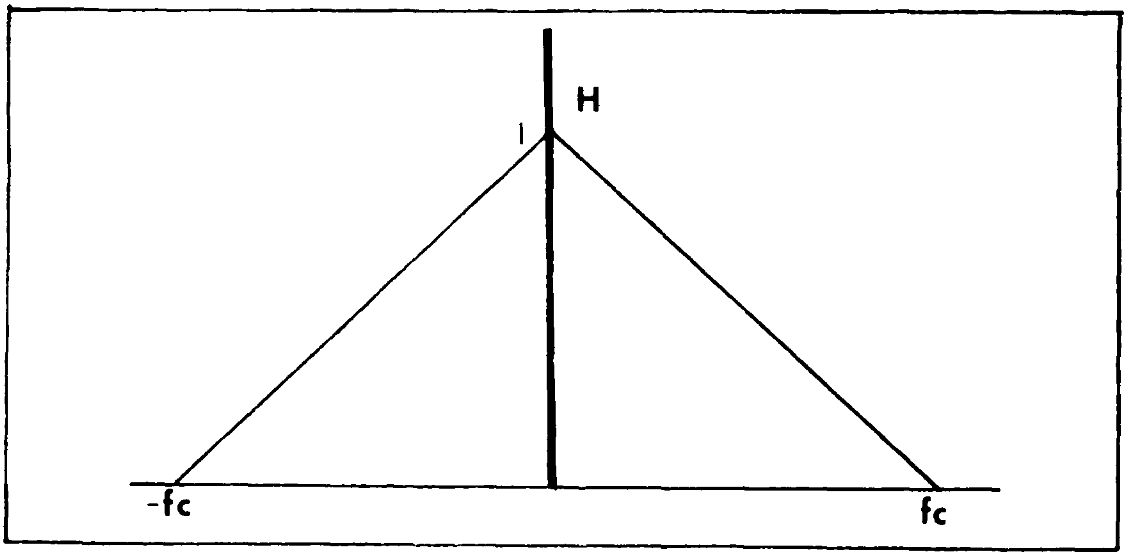

Figure 4. OTF of P = Rect(x)

the object from the spectral parameters

$$FT^{-1}\left[G_i\right] = FT^{-1}\left[\frac{(G_o)}{(H)}\right] = I(xo) \tag{2.18}$$

The problem with resolution is in the use of limited apertures and noise, since limited apertures attenuate the high spatial frequency terms essential for high resolution and the noise terms are greatly magnified in the inverse process, as will be explained later. Larger pupils would alleviate much of the problem but there is a physical limit to the size of usable optical systems, especially for space applications.

In the next chapter, a particular matrix method for increasing resolution with limited spatial bandwidth will be examined. It will be shown that increased resolution can be achieved under certain conditions. By knowing a priori that the object is finite with a known maximum extent, and by using a smoothing parameter, the increase in resolution can be quite substantial.

III. Superresolution Scheme

Introduction

The purpose of this chapter is to develop a mathematical model for incoherent imaging with limited bandwidth optical systems. The limited bandwidth is realized by symmetric multiple apertures as well as the traditional low pass (in spatial frequency) model. It has been speculated that for a limited bandwidth system, better resolution could be obtained using a bandpass aperture insead of the low pass system traditionally used (9). Multiple aperture systems consisting of relatively small, precise optical elements could simulate larger optical systems which are costly and extremely hard to manufacture. The optical systems will be described in terms of its optical transfer function, H, and its exit pupil, P. The mathematical model uses discrete values with vector and matrix analysis. For the purpose of this thesis, the truncation errors and sampling errors will not be discussed. The data is assumed to be adequately sampled and the truncation errors are considered to be negligible compared to the noise. This chapter describes the discrete solution to equation (2.18) using linear methods.

Math Model

To effectively model the imaging system, a priori knowledge of the object is of prime importance in reconstrucing the object from image data. The object is known to be finite within the first M units of the N bit object vector, x_o. The finite object can be represented by $\bar{D}\vec{x_o}$ where $\bar{D}$ is the diagonal matrix (all elements zero not on the diagonal)

$$\bar{D} = \mathrm{diag}(\underbrace{1,1,\ldots,1}_{M},\underbrace{0,0,\ldots,0}_{N-M}) \tag{3.1}$$

The matrix $\bar{D}$ is known as the spatial truncation matrix. The spatial truncation matrix has been zero-filled to an N x N matrix to match the order of subsequent matrices.

The N bit discrete Fourier transform (DFT) of the truncated object is

$$\mathrm{DFT}(\vec{x_o}) = \bar{F}\bar{D}\vec{x} \tag{3.2}$$

and $\bar{F}$ is the matrix representing the Fourier transformation, DFT, whose components are

$$\bar{F}(m,n) = \exp(-j2\pi mn/N) \tag{3.3}$$

$$\text{for } m,n = 0,N-1$$

Thus, $\bar{F}$ is a complex, N x N matrix.

In any optical optical system the pupil is finite and passes only a limited number of spatial frequency terms. In an incoherent imaging system, the transfer function is the autocorrelation of the pupil function, as derived in chapter two. Since only a finite number of spatial frequency terms will pass through the optical system, the filtering effect, or transfer function, can be represented by the diagonal matrix B, whose diagonal components contain the appropiate attenuation factors. The matrix B is equal to

$$B = \mathrm{diag}(DC, f_1, f_2, \ldots, f_c, 0, 0, \ldots 0, f_c, \ldots f_2, f_1) \qquad (3.4)$$

where DC is the DC coefficient, the f_i's are the various spatial frequency coefficients, and f_c is the cutoff frequency (highest spatial frequency passed by the system). The symmetry of the $\bar{B}$ matrix is the same as the symmetry of the forthcoming DFT's. For appropiate multiplication of vectors and matrices, either the $\bar{B}$ matrix is changed to the symmetry of the DFT (which it is) or the DFT is rearranged to the symmetry of th $\bar{B}$ matrix. Thus, the spatial frequency representation of the image is $\bar{B}\bar{F}\bar{D}\vec{x}_o$. The diagonal elements of $\bar{B}$ are obtained from the specific values obtained from calculating $\vec{P}**\vec{P}$. In this thesis, all pupils will be centered and symmetric about the optic axis. It is a property of discrete sequences that an N-bit sequence convolved with an M-bit sequence generates a sequence of length M+N-1 (15:12). Thus, for a pupil of length L, the transfer function response will be of length 2L-1. As an example, let $\vec{P}$ = (1 1 1 1)' (P is a column vector, so ' denotes transpose of the row vector). The convolution of $\vec{P}$ with itself will yield the diagonal elements of the matrix $\bar{B}$, since convolution with itself is autocorrelation.

$$\vec{P}**\vec{P} = \begin{bmatrix} 1 \\ 2 \\ 3 \\ 4 \\ 3 \\ 2 \\ 1 \\ 0 \end{bmatrix} \quad \text{rearranged} \quad \vec{P}**\vec{P} = \begin{bmatrix} 4 \\ 3 \\ 2 \\ 1 \\ 0 \\ 1 \\ 2 \\ 3 \end{bmatrix} \tag{3.5}$$

where $\vec{P}**\vec{P}$ has been rearranged to the same symmetry as the DFT in equation (3.2). In the example, the transfer function consists of seven elements which correspond to the DC term plus three positive and three negative spatial frequency terms. Therefore, the four bit pupil passes the first three spatial frequency terms plus the zero frequency or DC term.

So far, the image is represented as $\bar{B}\bar{F}\bar{D}\vec{x}_o$. The last step remaining is to convert the spectral representation of the image back to a conventional spatial representation. The normal, noise free, space domain image can be written as

$$\vec{x}_i = FT^{-1}\,\bar{B}\bar{F}\bar{D}\vec{x}_o \tag{3.7}$$

which physically can be expressed as

$$\vec{x}_i = \bar{A}\vec{x}_o + \vec{n} \tag{3.8}$$

where $\bar{A} = \overline{FT}^{-1}BFD$ and $\vec{n}$ is the Gaussian, white, and additive noise vector. The components of $\overline{FT}^{-1}$ (inverse Fourier transform matrix) are

$$\overline{FT}^{-1}(m,n) = \exp(2j\pi mn/N) \quad \text{for } m,n = 0,N-1 \tag{3.9}$$

$\overline{FT}^{-1}$ is also an N x N complex matrix.

Solving for $\vec{x}_o$ in equation (3.8) is the mathematical problem of the superresolution process, and thus is the heart of this thesis effort. Equation (3.8) represents the linear transformation of the irradiance from the object plane to the image plane. Also, the problem is compounded by the fact that the image, $\vec{x}_i$, is affected by noise, $\vec{n}$, in the imaging system. For this paper, the noise is considered to be Gaussian, white, and additive for all frequencies considered. The solution of $\vec{x}_o$ from equation (3.8) is not a trivial matter as the matrix A is severely ill-conditioned which can lead to serious problems in the solution of $\vec{x}_o$. A discussion of ill-conditioned matrices follows.

Properties of Ill-conditioned Matrices

The matrix $\bar{A}$ can be severely il-conditioned. Ill-conditioned matrices have the potential to cause very large errors when used to solve linear equations because of the propogation of errors. The length, or size, of a matrix, can be expressed as its norm or magnitude, and is expressed as

$$||\bar{A}||_2 = \text{Two norm of } \bar{A} \qquad (3.10)$$

where the two norm of $\bar{A}$ is the most restrictive norm (11:26). The two norm of a matrix is defined as the largest singular value (the singular values are represented as s_i, for $i = 1,k$ where k is the rank of the matrix) of that matrix. The singular values of a matrix are the square roots of the corresponding eigenvalues of the matrix. The condition number of a matrix, $c(\bar{A})$, is a measure of the stability of the matrix. The condition number of the matrix $\bar{A}$ is defined as

$$c(\bar{A}) = ||\bar{A}||_2 \times ||\overline{A^{-1}}||_2 \qquad (3.11)$$

where the magnitude of $\bar{A}^{-1}$ is equal to the inverse of the smallest singular value of $\bar{A}$ (12:166).

As an example, let $\bar{A}$ be the 32 x 32 matrix obtained from (see Appendix B):

$\vec{P}$ = (1111100000011111)' and

$\bar{D}$ = Diag(1,...1), for M = 32

where ' denotes transpose since $\vec{P}$ is a column vector. From the data table, the largest singular value of $\bar{A}$ is 320 and the smallest singular value is 1.46 E-4. Since the magnitude or two norm of $\bar{A}$ is equal to 1/(1.46 E-4), the condition number is roughly 2E+10. Why is the condition number important? The importance of the condition number is

The condition number is a measure of stability in that it gives an upper bound on the possible magnitude of error in the solution of the matrix equation $\bar{A}\vec{y} = \vec{b}$, for $\bar{A}$ the image matrix, $\vec{y}$ the object, and $\vec{b}$ the noisy object. Let e(y) represent the potential error possible from the solution of $\vec{y}=\bar{A}^{-1}\vec{b}$, and let e(b) represent the error present in $\vec{b}$, the Gaussian noise. The relative error in the solution for $\vec{y}$ will have the upper bound expressed by

$$e(y) <= c(\bar{A}) \times e(b) \tag{3.12}$$

For the example cited above, the condition number was approximately 2E+7, so the relative error limits can be expressed as

$$e(y) <= 2E+7 \times e(b) \tag{3.13}$$

where e(b) is usually expressed as the noise variance. It is important to realize that the limit to the error is an upper bound on the error and that not every component of the solution vector will be in error by this amount, but each component could be in error by this amount. The use of condition numbers to test matrices for stability is a figure of merit type relationship. For good linear systems, the condition number should be small. By using the two norm, the most restrictive error potential was achieved. Other, simpler norms could have been used, but generally lead to higher condition numbers. Another way of looking at condition numbers is to say that a matrix with a large condition number is an almost singular matrix, meaning that the matrix inversion is quite suspect. From linear algebra, a unique solution to a matrix transformation is only possible when the inverse to the matrix exists. Therefore, solving a linear system of equations with an almost singular matrix means that the matrix is not very stable and can cause large errors in the solution.

Least Squares Solution

The problem of imaging can be restated as

$$\bar{A}\vec{x}_o \cong \vec{x}_i \tag{3.14}$$

where $\cong$ implies that a least squares solution is being sought. The notation uses x_{ii} as the ith component of the vector $\vec{x}_i$. The least squares solution minimizes the difference expressed by

$$\|\bar{A}\vec{x}_o - \vec{x}_i\|_2 = \text{error} \tag{3.15}$$

where the subscript 2 represents the 2 norm of the vector, also known as the Euclidean distance, as shown in equation (3.16).

$$\|\vec{x}\|_2 = \sqrt{(x_1)^2 + (x_2)^2 + \ldots (x_n)^2} \tag{3.16}$$

To implement the least squares solution, the matrix $\bar{A}$ must be decomposed into a product of a diagonal matrix and two orthogonal matrices. The components of the diagonal matrix will be the singular values of $\bar{A}$. The matrix $\bar{A}$, where $\bar{A} = \bar{F}\bar{T}^{-1}\ \bar{B}\bar{F}\bar{D}$, can be rewritten as a product of three matrices (12:237)

$$\bar{A} = \bar{U}\bar{S}\bar{V}' \tag{3.17}$$

where $\bar{U}$ is an N X N orthogonal matrix, and $\bar{V}'$ is an L X L orthogonal matrix. $\bar{S}$ is an N X L orthogonal matrix whose diagonal elements are the singular values of A and are in decreasing order. $\bar{S}$ looks like

$$\bar{S} = \mathrm{Diag}(s_1, s_2, s_3, \ldots, s_m, 0.0 \ldots 0) \tag{3.18}$$

where $s_1 > s_2 > s_3 > \ldots > s_m$. There are only M singular values since $\bar{D}$ reduces the rank of $\bar{A}$ to M.

The least squares method of solving linear equations serves to minimize the two norm of the difference vector as expressed in equation (3.16). Substitute for $\bar{A}$ in (3.15) to obtain

$$\|\bar{U}\bar{S}\bar{V}'\vec{x}_o - \vec{x}_i\|_2 = \text{error} \tag{3.19}$$

where $\bar{A}=\bar{U}\bar{S}\bar{V}'$. Since $\bar{U}$ is orthogonal, $\bar{U}\bar{U}' = \bar{I}$, where $\bar{I}$ is the identity matrix. By multiplying each term by $\bar{U}'$, the expression becomes

$$\|\bar{S}\bar{V}'\vec{x}_o - \bar{U}'\vec{x}_i\|_2 = \text{error} \tag{3.20}$$

where the error is the same, since multiplying a vector by an orthogonal matrix does not magnify the norm of the vector(12:282). By substitution, equation (3.20) becomes

$$\|\bar{S}\vec{y} - \vec{b}'\|_2 = \text{error} \tag{3.21}$$

where $\vec{y}=\bar{V}'\vec{x}_o$ and $\vec{b}'=\bar{U}\vec{x}_i$. Therefore, $\vec{x}_o$ solves the least squares problem (3.15) if and only if $\vec{y}=\bar{V}\vec{x}_o$ solves

$$\|\bar{S}\vec{y} - \vec{b}'\|_2 = \text{minimum error} \tag{3.22}$$

Since $\bar{S}\vec{y}$ is a diagonal matrix composed of the singular values of $\bar{A}$ times y_i, the difference vector of (3.15) can be expressed as

$$\|\bar{S}\vec{y} - \vec{b}'\|_2 = \left[(s_1 y_1 - b_1')^2 + \ldots (s_m y_m - b_m')^2 + b'^2_{m+1} + \ldots b'^2_n\right]^{\frac{1}{2}} \tag{3.23}$$

The minimum error solution satisfies

$$s_i(y_i) - b_i = 0 \text{ or } y_i = b_i/s_i \tag{3.24}$$

for all values of i. By back substitution,

$$y_m = b'_m / s_m = \sum_{j=1}^{L} \bar{U}'(m,j)\ x_{ij}\ (1/s_j) \qquad (3.25)$$

and since $\vec{y} = \bar{V}'\vec{x}_o$

$$\vec{x}_o = \bar{V}\vec{y} \qquad (3.26)$$

since $\bar{V}$ and $\bar{V}'$ are orthogonal matrices. By substituting for $\vec{y}$ in equation (3.26), the mth component of $\vec{x}_o$ is

$$(x_o)_m = \sum_{K=1}^{L} \bar{V}(m,k) \sum_{j=1}^{L} \bar{U}'(m,j)(x_{ij})\ (1/s_j) \qquad (3.27)$$

which can be rearranged to yield

$$(x_o)_m = \sum_{K=1}^{L} \sum_{j=1}^{L} \bar{U}'(m,j)(x_{ij})\ (1/s_j) \bar{V}(m,k) \qquad (3.28)$$

By using vector notation, equation (3.27) and (3.28) can be rewritten as

$$\hat{x}_o = \sum_{j=1}^{L} (1/s_j)(\vec{x}_i \cdot \vec{u}^j)\vec{v}^j \qquad (3.29)$$

where $\vec{u}^j$ and $\vec{v}^j$ are the left and right singular vectors obtained from the jth column of the matrices $\bar{U}$ and $\bar{V}$ respectively. The solution vector, $\hat{x}_o$, denotes a least squared solution, and • is the dot product operator. This solution is also referred to as the inverse filtering solution, since the least squares solution serves to reverse the matrix operation and return the original (object) vector in our specific application (14:205).

Modifications to Least Squares Method

Since there are very small singular values in the matrix $\bar{A}$, the presence of noise will greatly reduce the effectiveness of the least squares solution in the high order terms. By using the method of Rushforth, et al, (14), $1/s_K$ is replaced with an appropiate smoothing or regularization function to attenuate the high order terms and pass the lower order terms unchanged. The smoothing function serves to avoid overamplification of the higher order noise terms. For this thesis, $1/s_K$ is replaced with $f(s_K)$, where

$$f(s_K) = \frac{s_K^3}{s_K^4 + \alpha} \qquad (3.30)$$

Choosing an appropiate α prevents overamplification of the high order noise terms. α was chosen in most cases to be 10E-10 as this provided adequate attenuation with respect to the smaller singular values. Various other smoothing functions and concepts could be considered. The basic concept is to reject those higher order terms knowing as much about the object as possible beforehand. To get high resolution, some high order terms must be present in the solution. Therefore, if the object is known beforehand to be less than 10 units long, the spatial truncation matrix, $\bar{D}$, solution. Therefore, if the object is known beforehand to be less than 10 units long, the spatial truncation matrix, $\bar{D}$, will be finite for only 9 elements. By truncating at nine elements, the matrix $\bar{A}$ will be of rank less than or equal to nine, so there will be only nine singular values, thus the lower singular values will already be rejected (12:336).

The following chapter will describe the computer program and computational algorithms used to implement the least squares solution.

IV. Computer Model

Introduction

The purpose of this chapter is to describe the analytical implementation of the least squares superresoslution scheme as described in the previous chapters. The computer system used was a VAX 11/785 utilizing the VMS 4.1 operating system. The subroutines used for convolution, Gaussian random number generation, and singular value decomposition of matrices were from the International Mathematical and Statistical Subroutine Library (IMSL) (10). The matrix multiplication routines were written by the author. The program was written using standard Fortran 77 (18).

Figure 5. is a flowchart depicting the superresolution process as described in the previous chapter. Refer to this figure throughout the chapter for reference. A complete listing of the program, SRES, is contained in the appendix.

Computer Model

The following variables are defined for convenience.

L = pupil length (integer)
N = dimension of square matrix A (integer)
M = finite, known extent of object
$\underset{\sim}{\alpha}$ = smoothing coefficient (real exponential)
$\vec{P}$ = pupil vector
DSEED = double precision constant
s_j = jth singular value (real)
$\underline{*}$ = convolution operator
$\underset{\sim}{Q}$ = matrix named Q
$\bar{r}$ = vector named r
r_i = ith component of r

$\bar{A}^{-1}$ = inverse of matrix $\bar{A}$
$\bar{A}'$ = transpose of matrix $\bar{A}$
SNR = power signal to noise ratio
PSEQ = power in discrete sequence
σ_n^2 = noise variance
$\bullet$ = dot product operator

The first variable to define is N, dimension of the transfer matrix, $\bar{A}$. The criterion for N was that it be large enough to model an imaging system but small enough to operate efficiently with the computer. Also, N was chosen to be a power of two, since this makes the system easier to work with, with respect to the IMSL subroutines. N was chosen to be 32 for all configurations. By choosing a value for N, the values for M and L are somewhat restricted. The length of the pupil, L, must be less than or equal to N/2, since the matrix $\bar{B}$ is composed of elements of $\vec{P}*\vec{P}$ and convolution of two vectors lenghens the resulting vector. Also, the object dimension, M, cannot be larger than N because of the matrix vector multiplication scheme.

The computer program is interactive and prompts the operator to input values for L, M, SNR, DSEED, and α. The operator is then prompted to enter values for the pupil vector and object vector. The program uses the pupil vector to generate the $\vec{P}*\vec{P}$ vector which in turn provides the elements of the diagonal matrix, $\bar{B}$. The IMSL subroutine VCONVO performs the necessary convolution. The values for M and N are sufficient to create the matrices $\bar{F}$ (Fourier transform matrix), $\overline{FF}$ (inverse Fourier transform matrix), and $\bar{D}$ (spatial truncation matrix of M diagonal elements). With the matrix $\bar{B}$ available, the matrix product $(\overline{FF})(\bar{B})(\bar{F})(\bar{D}) = \bar{A}$ ($\bar{T}$ in program SRES) can be calculated. After the matrix $\bar{A}$ is calculated, the product $\bar{A}\vec{x}_o$ can be calculated to yield the noise free image. With the noise free image available, the noisy image can be calculated.

The operator has already input the value for the signal to noise ratio (SNR) which can be used with the noise free image to create a noisy image. The noise is assumed to be Gaussian, white, and additive for all spatial frequencies. The definition of SNR is

$$SNR = \frac{PSEQ}{\sigma_n^2} \tag{4.1}$$

which means that

$$\sigma_n^2 = \frac{PSEQ}{SNR} \tag{4.2}$$

where the noise variance is represented as σ_n^2 and PSEQ is the power in the image sequence. The power in the vector $\vec{x}$ is defined as

$$PSEQ = (1/M) \sum_{k=1}^{M} (x_k)^2 \tag{4.3}$$

where the vector is of length M. The noise variance, σ_n^2 , is the power in the noise vector $\vec{x}_n$ and is defined as shown in equation (4.3). The noise variance assumes a zero mean. The variance is also equal to the square of the standard deviation of the noise distribution. With SNR being provided by the operator, the variance can be calculated from equation (4.2). Using the IMSL subroutine GGNML and the value of the variance, the Gaussian noise vector is generated. The noise is amplitude at this point, so each term is squared for power and added termwise to the original noiseless image to create the noisy image. At this point, the least squares process can be implemented. After the matrix $\overline{A}$ ($\overline{T}$ in computer program) has been created, the IMSL subroutine LSVDF is used to create the three matrices, $\overline{U},\overline{S},\overline{V}'$, which are to be used in the superresolution process. After the singular values have been generated, the substitution for $1/s_k$ is implemented using the smoothing parameter, α, to negate the effects of the very small singular values of $\overline{A}$.

As can be easily seen, the computer program performs the exact operations described in chapter III. In the next chapter, the results for various pupil configurations and parameter values will be examined. It will be shown that the least squares method with a priori knowledge can resolve two incoherent point sources not ordinarily resolved in a conventional low pass imaging system.

SRES Computer Program

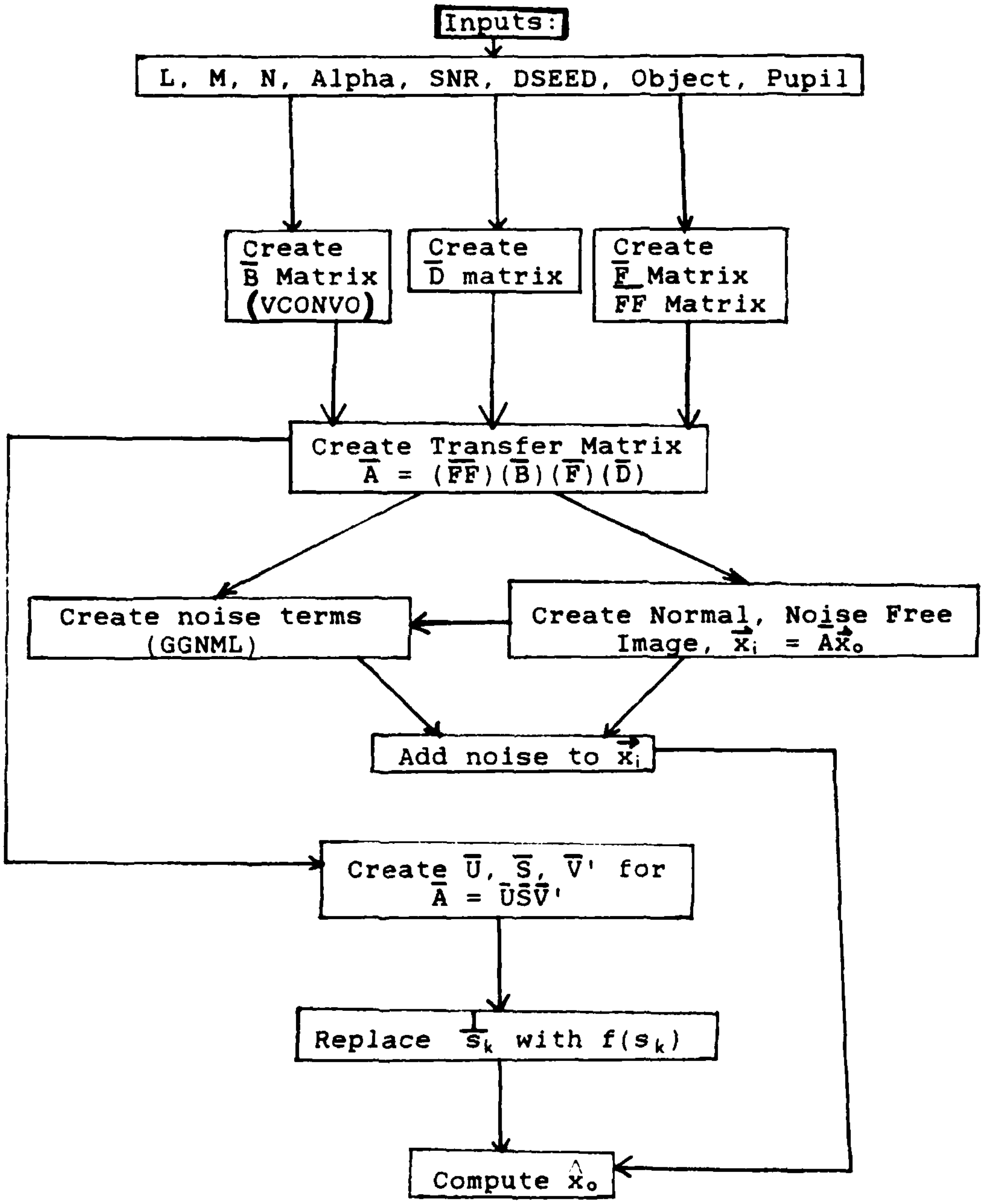

Figure 5. Superresolution Flow Chart

V. Results and Conclusions

Introduction

This chapter presents the results and conclusions obtained using the computer program SRES to simulate superresolution using the least squares method outlined in the previous chapters. In review, 1/2 P is one-half of the symmetric pupil function of length L, where L <= 16. M is the assumed or known maximum length of the object, where M <= 32 since N=32 is the square dimension of the transfer matrix A (T in SRES). SNR is the signal to noise ratio and is the smoothing or regularization constant used to attenuate the effect of the very small singular values. The error used throughout this chapter is the Euclidean distance or two norm of the difference vector between the object and noisy image where the image is the superresolved image. The effects of the different parameters will be investigated and discussed. After the results are presented, a conclusion section will close out the formal portion of this thesis. Also, pupil function performance for various pupils is contained in appendix B.

Results

Band-Pass vs Low-Pass Pupil. Both pupils considered contained six apertures corresponding to the six elements of the pupil vector. The low pass half-pupil was (00000111)', and the high pass half-pupil was (11100000)'. Both pupils column vectors as denoted by the transpose symbol. The modulation transfer functions (MTF) for each of these pupils is shown in Fig. 6. As can be seen, the band-pass pupil passes higher frequency components than the low-pass pupil. The band-pass pupil passes the higher spatial frequency terms needed to resolve the two incoherent point sources located closer than the normal resolution distance. Figure 7 illustrates the effect of using the high-pass pupil instead of the low-pass pupil for superresolution. By using the band-pass pupil, the superresolution scheme served to separate the two incoherent point sources, with only two small (40%) side lobes present. By using a threshold detection criteria, the high pass pupil can superresolve the object consisting of the two incoherent point sources using the least squares method and a smoothing function, while the low pass pupil cannot superresolve the object.

Effect of A Priori Knowledge. Figure 8 illustrates the importance of a priori knowledge using the superresolution algorithm. By using the low-pass pupil shown, the normal image does not resolve the two incoherent point sources (object) of Figure 7-a). The superresolution scheme is able to resolve the object only at M=8, where M is the a priori knowledge that the object was less than or equal to 8. The effects are quite interesting for M=16, as the algorithm tries to restore the object, but there is insufficient information to do so. Figure 11 presents a plot of M vs Error for the five various pupil functions at a

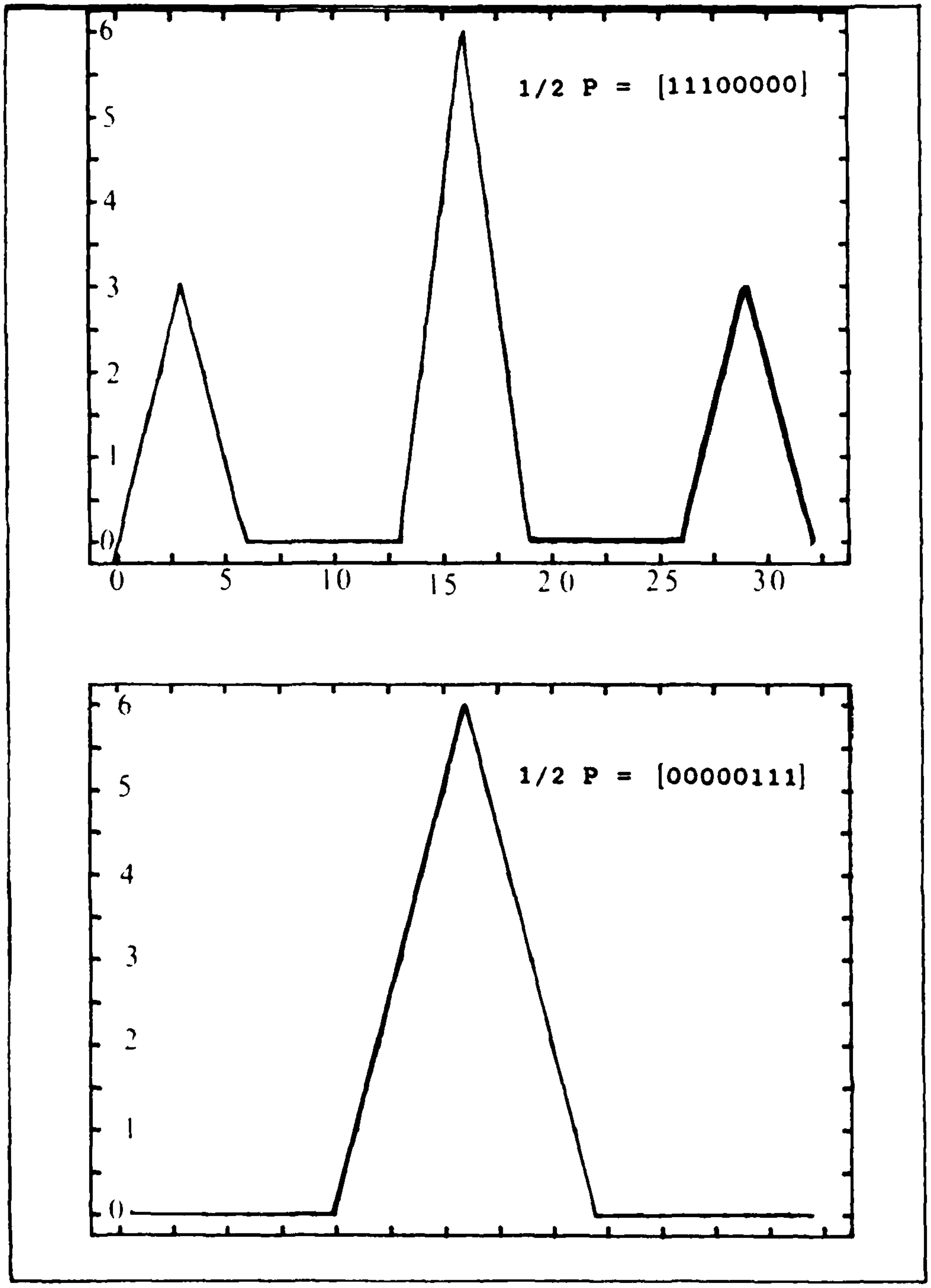

Figure 6. Examples of Modulation Transfer Functions

insufficient information to do so. Figure 11 presents a plot of M vs Error for the five various pupil functions at a constant SNR =100. As can be seen, the known information concerning the object does reduce the error in many cases. It is interesting to notice that in some cases, the error is almost constant for the values of M up to the bend in the curve. The error for P3, P4, and P5 are all fairly constant up to M=24. The smaller pupils exhibit similiar responses for smaller values of M. It is important to define the object domain as close as possible in order to achieve reliable and accurate results.

Effect of α. Figure 9 illustrates the effect of the smoothing parameter, α. As can be seen, holding all parameters but constant, the higher values for (10E-5,10E-10) serve to resolve the object quite well with a rather limited pupil. As α aproaches zero, the effect of the noise due to the ill-conditioned nature of the system is obvious. As can be seen, the processed images using very small values for α are quite haphazard and look nothing like the original object, even with the high SNR=100. Due to the nature of the imaging problem, the superresolution alogorithm must use a good estimate for the smoothing parameter, α , in order to achieve accurate results.

Effect of Noise. Figure 10 serves to illustrate the effects of noise on the superresolution technique using the least squares method with a smoothing parameter. The superresolved images all appear to be the same, illustrating the noise resistant nature of the superresolution algorithm. Figure 12 also shows the noise resistance of the least squares method. For SNR equal to 100, 50, and 5; the error vs pupil size is almost equal for each pupil. Only at the high SNR of 2 does the noise dominate. This algorithm has proved to be quite good in the presence of moderate noise.

Error Analysis. Figures 10 and 11 illustrate the sources of error present using the least squares method for superresolution. The error is expressed as the distance between the object and superresolved image, using the Euclidean distance, or two norm.

In Figure 10, the error is plotted on the vertical axis and the pupils are plotted on the horizontal axis. In this graph, all pupils are the high pass versions with P1 consisting of 6 elements, P2 consisting of 8 elements and so forth with the last pupil, P5 consisting of 14 elements. Each curve is at a constant SNR. The error is seen to decrease as the pupil elements are increased. This is logical, since the more pupil elements available, the more spatial frequencies passed by the system, resulting in more information available for the algorithm.

In Figure 11, the effect of a priori information is analyzed. The known extent of the object, M, is plotted versus error for constant pupils. At the extreme, with the object known to be within 32 bits, the larger pupils have the

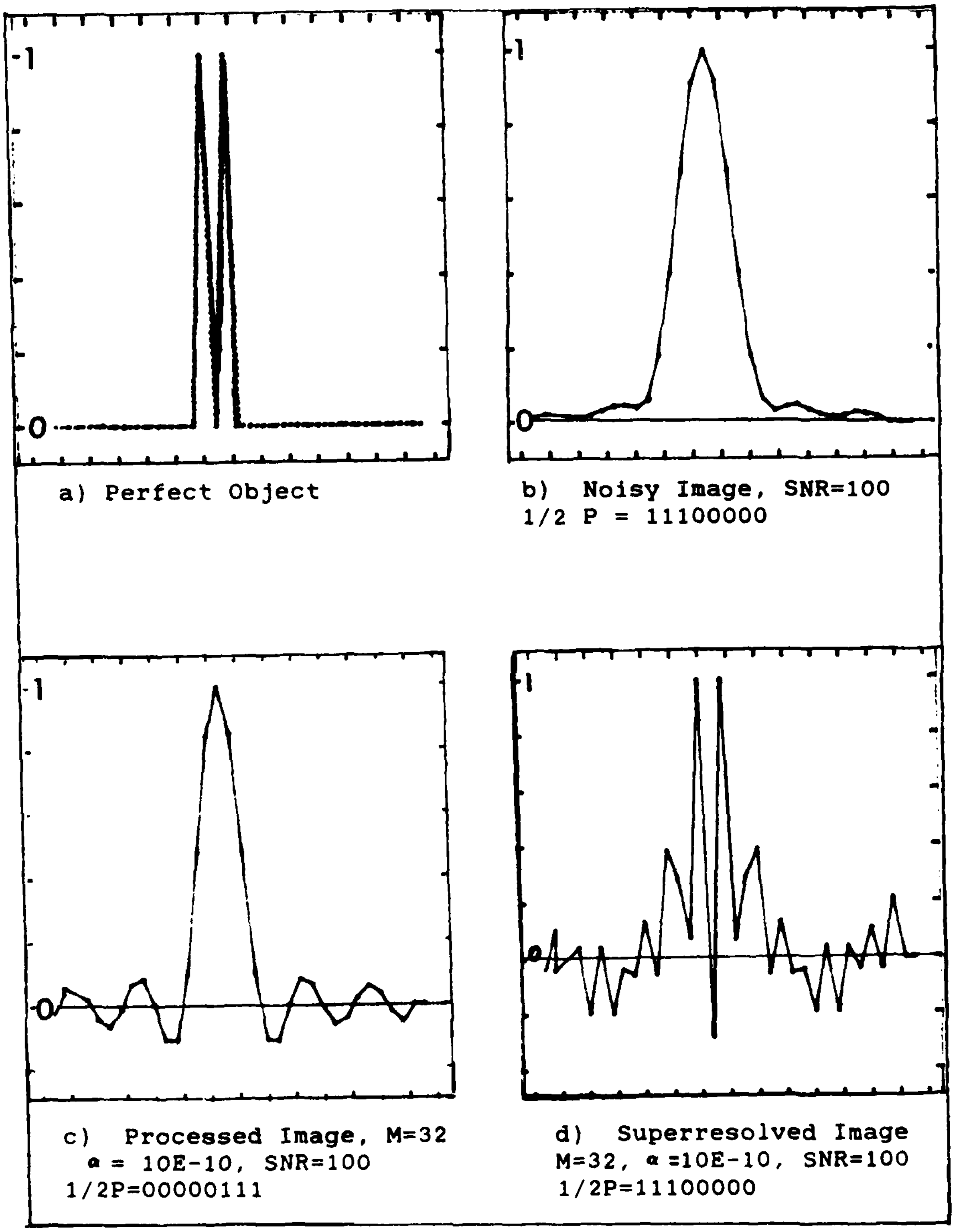

a) Perfect Object

b) Noisy Image, SNR=100
1/2 P = 11100000

c) Processed Image, M=32
α = 10E-10, SNR=100
1/2P=00000111

d) Superresolved Image
M=32, α =10E-10, SNR=100
1/2P=11100000

Figure 7. Superresolution Example #1

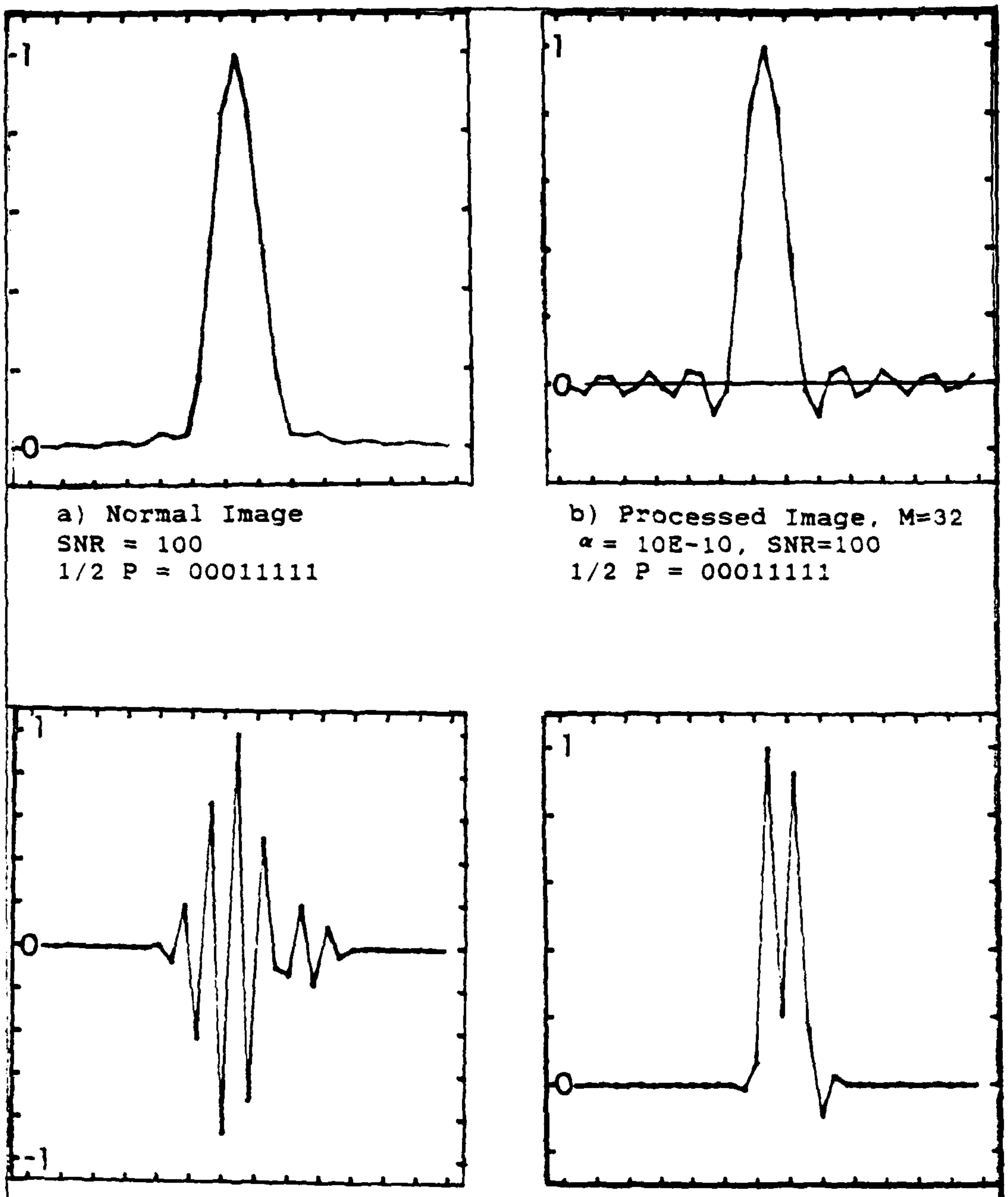

a) Normal Image
SNR = 100
1/2 P = 00011111

b) Processed Image, M=32
α = 10E-10, SNR=100
1/2 P = 00011111

c) Processed Image, M=16
α = 10E-10, SNR=100
1/2P=00011111

d) Superresolved Image
M=8, α = 10E-10, SNR=100
1/2P = 00011111

Figure 8. Superresolution Example #2

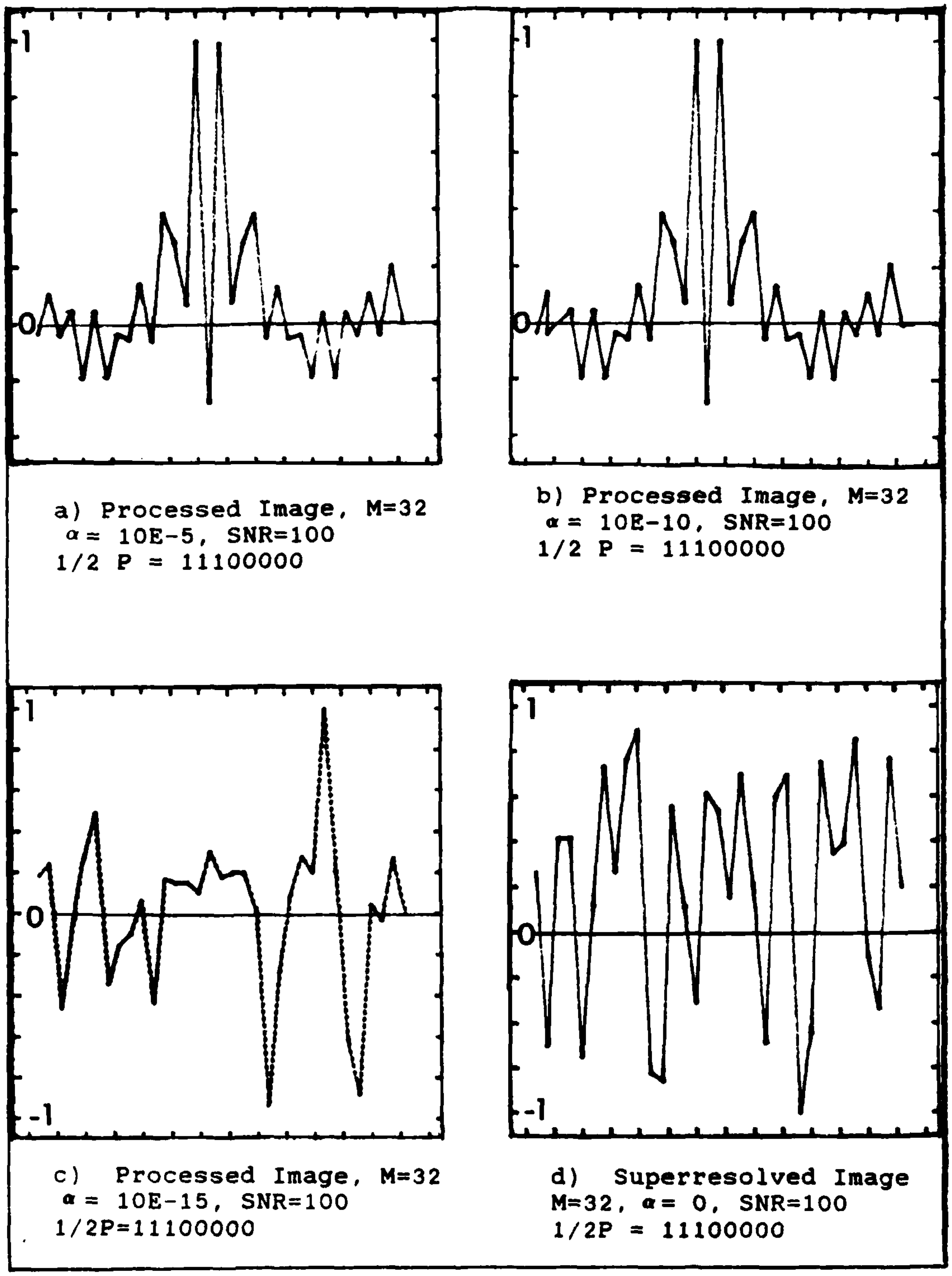

a) Processed Image, M=32
α = 10E-5, SNR=100
1/2 P = 11100000

b) Processed Image, M=32
α = 10E-10, SNR=100
1/2 P = 11100000

c) Processed Image, M=32
α = 10E-15, SNR=100
1/2P=11100000

d) Superresolved Image
M=32, α = 0, SNR=100
1/2P = 11100000

Figure 9. Superresolution Example #3

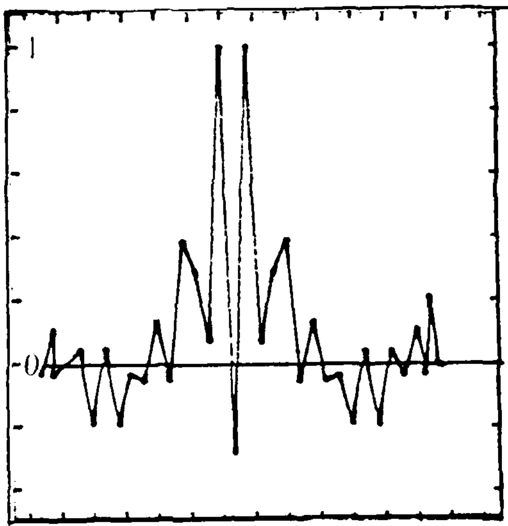

a) Processsed Image M=32
α = 10E-10, SNR=100
1/2P = [11100000]

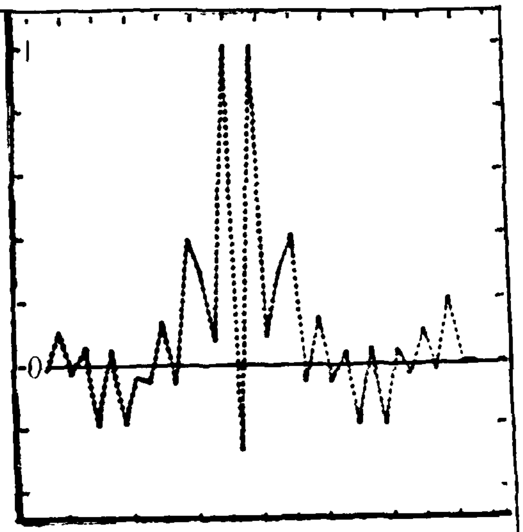

b) Processed Image, M=32
α = 10E-10, SNR=50
1/2 P = [11100000]

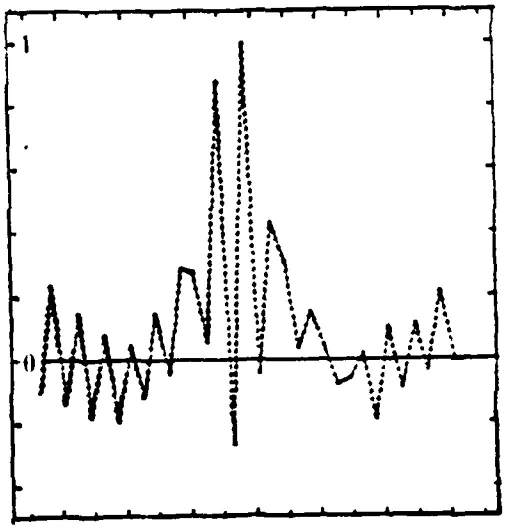

c) Processed Image, M=32
α = 10E-10, SNR=5.0
1/2 P = [11100000]

Figure 10. Superresolution Example #4

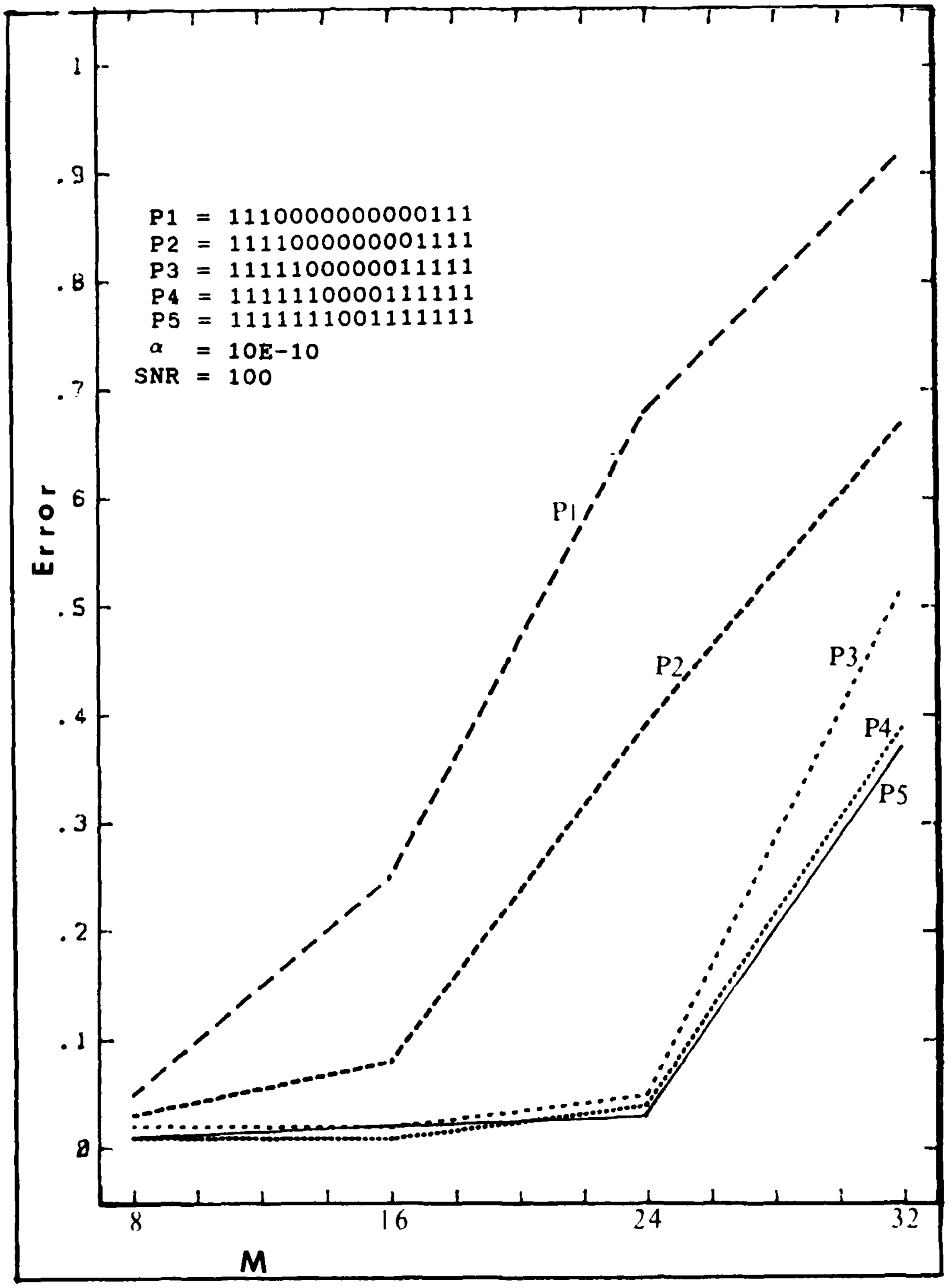

Figure 11. Error vs Known Length of Object

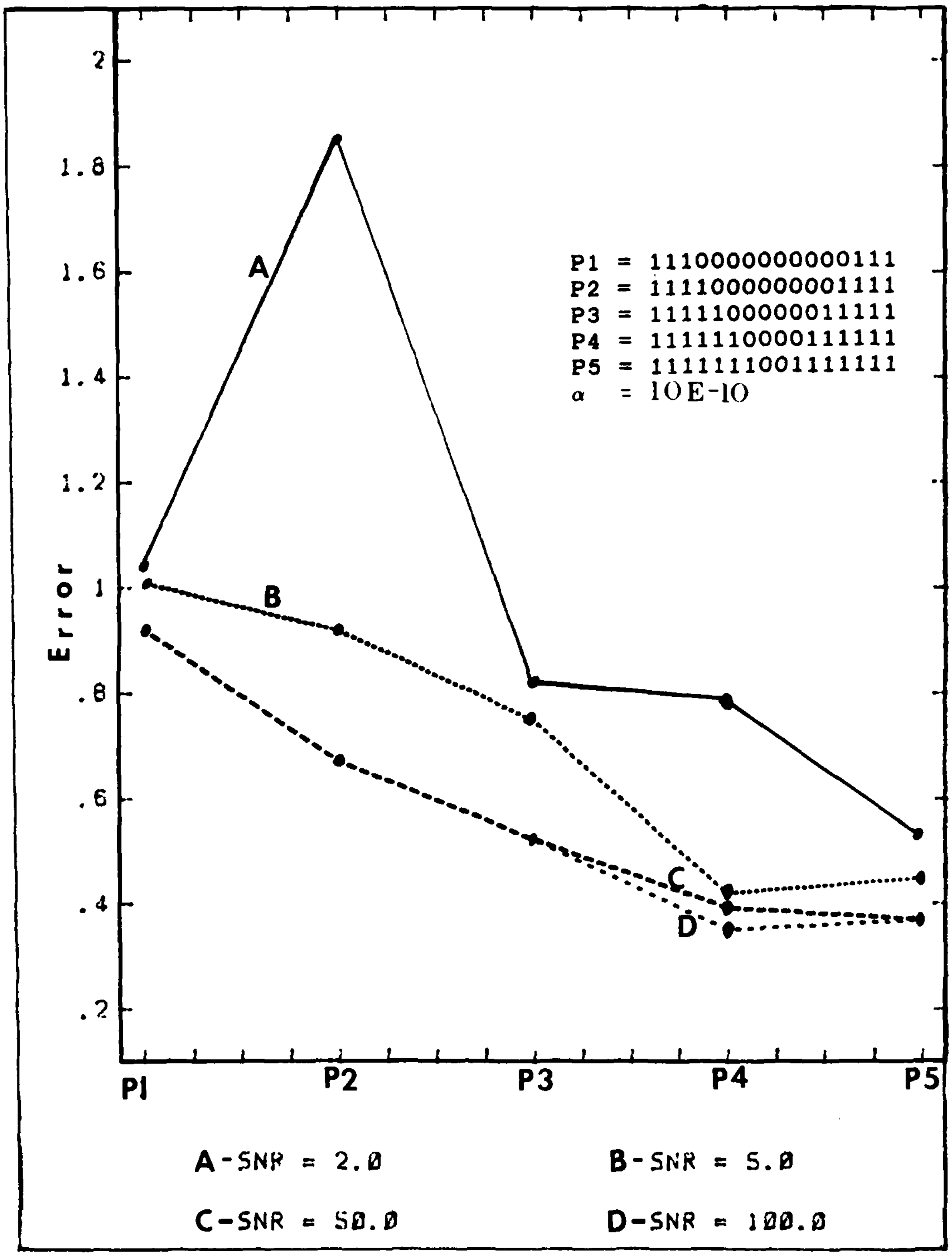

Figure 12. Error vs Size of Pupil

least error, which is logical. As the known extent of the object increases, or as M decreases, the error decreases, with the larger pupils approaching the constant level quite rapidly. For the 10, 12, and 14 bit pupils, the error is constant up to M=24, while the 6 and 8 bit pupils decrease at different rate that appears almost linear. The effect of M is obvious, but as can be seen from some of the pupils, the increase in information concerning the maximum extent does not yield appreciable results concerning error reduction. As an example, for P3 consisting of 10 bits, the error for M=24 is about the same as for M=8. For P3, the information gained by knowing that M=8 instead of at least 24 is slight. The error is seen to be almost linear over some range, and almost flat up to a threshold level.

Conclusions

Based on the performance of the computer simulation, superresolution is achievable in limited bandwidth optical systems. The performance of the superresolution process is affected by:

A priori information available concerning the object
Type of pupil
And noise in the system.

By using a smoothing parameter, α, the overamplification of the high order noise terms is avoided. With finite precision arithmetic and noise, the very small singular values of the transfer matrix must be attenuated in order to preserve the identity of the original object. The problem with attenuating the high order singular values is that these singular values correspond to the high order spatial frequency terms needed for resolution. Obviously some high order terms are necessary for resolution, but amplification of the noise breaks down the superresolution process when high order singular values are present. For this one-dimensional case, the pupil was assumed to be symmetric and quite limited with a maximum length of 16. For a more rigorous approach, the pupil length could be increased, but the resulting increase in computer complexity would be quite costly. The results obtained graphically and in Appendix B illustrate the importance of the different parameters and verify the premise that high pass or band pass pupils will image better with this particular superresolution algorithm than low pass pupils of the same bandwidth. By knowing as much as possible about the noise and object, superresolution is achievable and possible using the least squares method.

Appendix A: Computer program listing for computer program SRES.

```
      PROGRAM SRES
C     A IS THE PUPIL VECTOR OR LENGTH LA, LA=LB SINCE
C     A IS CONVOLVED WITH ITSELF
C     PUPIL MUST BE <= 16, SINCE MAX=32 TOTAL
C     IWK IS A WORK VECTOR OF LENGTH M+1
2     FORMAT(E10.0)
3     FORMAT(I3)
4     FORMAT(' ALPHA =',E10.1)
5     FORMAT(F8.4)
6     FORMAT(' INPUT # OF PUPIL BITS IN A, THE PUPIL')
7     FORMAT(' PSEC= ',F10.4)
8     FORMAT(' INPUT MAX SIZE OF OBJECT SPACE, <,= TO N')
9     FORMAT(' ENTER PUPIL ELEMENT',I3)
12    FORMAT(' ALPHA =?, USE EXPONENTIAL FORM')
13    FORMAT(' N,L,M =',I3,1X,I3,1X,I3)
14    FORMAT(I3,F6.2)
15    FORMAT(F14.4)
16    FORMAT (' L BIT PUPIL VECTOR, INPUT L')
17    FORMAT (' SNR =',1X,F5.1)
18    FORMAT(' INPUT SIGNAL TO NOISE RATIO')
19    FORMAT(' INPUT DSEED')
20    FORMAT(' ')
22    FORMAT(F8.4)
25    FORMAT(' DSEED =',F12.3)
123   FORMAT(' ENTER OBJECT',I3)
142   FORMAT(I3,1X,E10.3,F6.2,F6.2,1X,5(1X,F8.4))
149   FORMAT(' PROCESSED IMAGE ERROR =  ',F10.5)
177   FORMAT('SV P P*P OBJ NOR IM NOISE NOI IM NEW IM')
178   FORMAT(' ')
209   FORMAT(' NOISY IMAGE ERROR =',F10.5)
      DIMENSION A(512),B(256),IWK(10),F(256),D(256,256)
      DIMENSION XI(256),XO(256),XX(256),SS(256),YY(256)
      DIMENSION PP(256,256),RR(32),R(32),CC(32),XCC(256)
      DOUBLE PRECISION DSEED,DDSEED
      COMPLEX SUM
      COMPLEX F(256,256),FF(256,256),FD(256,256)
      COMPLEX FFD(256,256),H(256,256)
      COMPLEX HH(256,256)
      DIMENSION T(32,32),UT(32,32),S(32),WK(64),SV(32)
      WRITE (6,20)
      WRITE (6,16)
      READ (5,3)L
      IC=L
C     N IS THE RANK OF THE TRANSFER MATRIX
      N=32
C     INPUT MAX DIMENSION OF OBJECT, M
      WRITE(6,8)
      READ(5,3)M
      LA=L
C     INPUT SNR
      WRITE (6,18)
```

```
      READ (5,15)SNR
C     INPUT DSEED
C     DSEED IS INPUT VARIABLE FOR IMSL ROUTINE GGNML
C     DSEED INITIATES SEARCH FOR GAUSSIAN NOISE TERMS
      WRITE(6,19)
      READ (5,22)DSEED
      DDSEED=DSEED
C     INPUT ALPHA
      WRITE (6,12)
      READ (5,2)ALPHA
      PI=3.1415927
      LB=LA
C     INPUT PUPIL ELEMENTS A(I)
      DO 33 I=1,L
            WRITE (6,9)I
            READ (5,3)A(I)
33    CONTINUE
      DO 34 I=(IO/2)+1,LA-IO/2
            A(I)=0.0
34    CONTINUE
C     SAVE PUPIL AS CC FOR LATER, LET B=A FOR CONVO.
      DO 48 I=1,L
            CC(I)=A(I)
            B(I)=A(I)
48    CONTINUE
C     CREATE P*P USING IMSL ROUTINE VCONVO
      CALL VCONVO (A,B,LA,LB,IWK)
      DO 53 I=1,N
            P(I)=0.0
53    CONTINUE
C     REARRANGE P*P TO MATCH SYMMETRY OF DFT
      DO 50 I=1,L
            P(I)=A(LA+1-I)
50    CONTINUE
      J=1
      DO 55 I=N-L+2,N
            P(I)=A(J)
            J=J+1
55    CONTINUE
      P(LA+1)=0.0
C     NOW MAKE PUPIL MATRIX PP (B IN THESIS)
C     MATRIX HAS PUPIL ELEMENTS ON THE DIAGONAL
      DO 65 I=1,N
            DO 65 J=1,N
            PP(I,J)=0.0
            IF(I.EQ.J)PP(I,J)=P(J)
65    CONTINUE
C     NOW MAKE TRUNCATION MATRIX D
C     M IS THE KNOWN MAX OF THE OBJECT
      DO 70 I=1,M
            DO 70 J=1,M
```

```
                  D(I,J)= 1.0
                  IF(I.NE.J) D(I,J)=0.0
70        CONTINUE
          IF (M.EQ.N) GOTO 155
          DO 75 I=M+1,N
                  DO 75 J=(M+1),N
                  D(I,J)=0.0
75        CONTINUE
155       WRITE(6,20)
C         NOW MAKE FT MATRIX AND FT INVERSE MATRIX
C         F IS FT AND FF IS INVERSE FT
          DO 88 I=0,N-1
                  DO 88 K=0,N-1
                  F(I+1,K+1)=CEXP(CMPLX(0.0,-2*PI*I*K/N))
                  FF(I+1,K+1)=CEXP(CMPLX(0.0,2*PI*I*K/N))
88        CONTINUE
C         NOW, WE HAVE OUR FOUR MATRICES, LETS MULTIPLY
C         FIRST MULTIPLE F AND D MATRICES
          DO 90 I=1,N
                  DO 90 J=1,N
                          SUM=(0.0,0.0)
                          DO 89 K=1,N
                          SUM=SUM+F(I,K)*D(K,J)
89        CONTINUE
          FD(I,J)=SUM
90        CONTINUE
C         F TIMES D STORED AS MATRIX FD, NOW MULTIPLY BY
C         MATRIX B WHICH IS THE PUPIL MATRIX PF
91        DO 95 I=1,N
                  DO 95 J=1,N
                  SUM=(0.0,0.0)
                          DO 98 K=1,N
                          SUM=SUM+PF(I,K)*FD(K,J)
98        CONTINUE
          PFD(I,J)=SUM
95        CONTINUE
C         BFD STORED AS PFD (NOTATION USED IN THESIS IS BFD)
C         NOW MULTIPLY BY INVERSE FOURIER MATRIX
92        DO 100 I=1,N
                  DO 100 J=1,N
                  SUM=(0.0,0.0)
                          DO 99 K=1,N
                          SUM=SUM+FF(I,K)*PFD(K,J)
99        CONTINUE
          HH(I,J)=(SUM)
100       CONTINUE
C         HH IS TRANSFER MATRIX
C         PSEQ IS THE AVG POWER IN THE SEQUENCE
C         ENTER OBJECT IRRADIANCE TERMS
          DO 124 I=1,M
                  XO(I)=0.0
```

```
124     CONTINUE
C       OBJECT IS TWO POINT SOURCES +/- 1 FROM OF AXIS
        XO(M/2-1)=1.0
        XO(M/2+1)=1.0
        PSEQ=0.0
C       NOW DO THE NORMAL IMAGE, IMAGE=T*OBJECT
C       T IS THE ABSOLUTE VALUE OF MATRIX HH
        DO 130 I=1,N
                DO 130 J=1,M
                T(I,J)=CABS(HH(I,J))
130     CONTINUE
        DO 120 I=1,N
                XX(1)=0.0
                        DO 117 J=1,N
                        XX(1)=T(I,J)*XO(J)+ XX(1)
117     CONTINUE
        XI(I)=XX(1)
120     CONTINUE
C       NORMALIZE IMAGE
        DO 101 I=1,N
        IF (XI(I).NE.0.0)SS(1)=XI(I)
        IF(SS(1).NE.0.0)GOTO 102
101     CONTINUE
102     DO 103 I=1,N
                IF(XI(I).GT.SS(1))SS(1)=XI(I)
103     CONTINUE
C       SS(1) IS MAX ABSOLUTE VALUE OF IMAGE
C       , NOW DIVIDE TO NORMALIZE
        DO 125 I=1,N
        XI(I)=XI(I)/SS(1)
        PSEQ=PSEQ+XI(I)
125     CONTINUE
        PSEQ=PSEQ/N
C       NOW DETERMINE NOISE VECTOR
C       SEE IMSL GGNML FOR DETAILS
C       NOISE IS AMPLITUDE SO SQUARE IT FOR POWER
C       SAVE ORIGINAL NOISELESS IMAGE AS XI(I)
C       NOISY IMAGE IS XOO(I)
        CALL GGNML(DSEED,N,R)
        DO 24 I=1,N
                RR(I)=(SQRT(PSEQ/SNR))*R(I)
                RR(I)=RR(I)*RR(I)
                XOO(I)=XI(I)+RR(I)
24      CONTINUE
C       NORMALIZE FINAL NOISY IMAGE XOO(I)
        DO 202 I=1,N
                IF(XOO(I).GT.SS1)SS1=XOO(I)
202     CONTINUE
        DO 203 I=1,N
                XOO(I)=XOO(I)/SS1
203     CONTINUE
```

```
C        UT IS AN N X N IDENTITY MATRIX ON INPUT
C        SEE IMSL LSVDF FOR INFO
         DO 132 I=1,N
                 DO 132 J=1,N
                         UT(I,J) = 0.0
                         IF(I.EQ.J) UT(I,J)=1.0
132      CONTINUE
C        NOW CREATE THE THREE MATRICES FROM T, T=USV'
C        SEE IMSL LSVDF FOR DETAILS
         CALL LSVDF(T,N,N,M,UT,N,N,S,WK,IER)
C        ON OUTPUT ,S(K) ARE SINGULAR VALUES
C         REPLACE S(K) WITH F(S(K))
C        THIS STEP REPLACES S(K) WITH F[S(K)]
C        AND PERFORMS THE DOT PRODUCT
C         WITH THE LEFT SINGULAR VECTOR FROM COLS OF UT
C        SAVE SINGULAR VALUES AS SV
         DO 136 K=1,M
                 SV(K)=S(K)
                 XX(K)=0.0
                 DO 134 I=1,N
                 XX(K)=XOO(I)*UT(K,I)+XX(K)
134      CONTINUE
         SS(K)=(S(K)*S(K)*S(K))/((S(K)*S(K)*S(K)*S(K))+ALPHA)
                 SS(K)=SS(K)*XX(K)
136      CONTINUE
C        MULTIPLY DOT PRODUCT X RIGHT SINGULAR VECTORS FROM T
C        YY(I) IS RECONSTRUCTED IMAGE
         DO 137 I=1,M
                 XX(I)=0.0
                 DO 138 J=1,M
                 XX(I)=XX(I)+T(I,J)*SS(J)
138      CONTINUE
         YY(I)=XX(I)
137      CONTINUE
C        NORMALIZE RECONSTRUCTED IMAGE
         DO 162 I=1,M
         IF(YY(I).NE.0.0)S(1)=ABS(YY(I))
         IF (S(1).GT.0.0) GOTO 163
162      CONTINUE
163      DO 164 I=1,M
         IF(ABS(YY(I)).GT.S(1))S(1)=ABS(YY(I))
164      CONTINUE
C        S(1) IS MAX ABS VALUE OF REC IMAGE
         DO 167 I=1,M
                 YY(I)=YY(I)/S(1)
167      CONTINUE
         WRITE (96,177)
         WRITE (96,178)
         WRITE(96,20)
         DO 139 I=1,N
         IF(I.GT.M)YY(I)=0.0
```

```
          IF(I.GT.L)CC(I)=0.0
          IF(I.GT.M)SV(I)=0.0
          IF (I.GT.LA+LB)A(I)=0.0
          WRITE(96,142)I,SV(I),CC(I),A(I),XO(I),XI(I),RR(I),XOO(I),YY(I)
135       CONTINUE
          SS(1)=0.0
          XX(1)=0.0
          DO 146 I=1,N
          XX(1)=XX(1)+(YY(I)-XO(I))**2
          SS(1)=SS(1) + (XOO(I)-XO(I))**2
146       CONTINUE
C         SS(1) IS THE EUCLIDEAN DISTANCE BETWEEN NOISY
C         OBSERVED IMAGE XOO(I)AND NOISE FREE OBJECT, XO(I)
C         XX(1) IS THE EUCLIDEAN DISTANCE BETWEEN THE
C         RESTORED IMAGE YY(I)AND THE ORIGINAL  OBJECT XO(I)
          SS(1)=SQRT(SS(1))
          XX(1)=SQRT(XX(1))
          WRITE (96,20)
          WRITE(96,20)
          WRITE (96,209)SS(1)
          WRITE (96,149)XX(1)
          WRITE (96,17)SNR
          WRITE (96,4)ALPHA
          WRITE(96,25)DDSEED
210       STOP
          END
```

Appendix B: Data from Computer Program SRES

Notes:

1. All objects are two incoherent point sources two bits apart
2. Processed image error (PIE) is the Euclidean distance (two norm of the difference) between the superresolved image and noise free object.

1/2 Pupil	SNR	M	ALPHA	PIE
00001111	100	32	10e-10	1.24
00001111	" "	24	" "	1.41
00001111	" "	16	" "	2.51
00001111	" "	8	" "	0.30
11111000	100	32	" "	0.52
11111000	50	""	" "	0.52
11111000	5	""	" "	0.75
11111000	2	""	" "	0.82
11111100	100	32	" "	0.39
11111100	50	""	" "	0.35
11111100	5	""	" "	0.42
11111100	2	""	" "	0.79
11111110	100	32	" "	0.37
11111110	50	""	" "	0.37
11111110	5	""	" "	0.45
11111110	2	""	" "	0.53
11111110	100	24	" "	0.03
11111110	100	16	" "	0.02
11111110	100	8	" "	0.01
11100000	100	32	0	3.28
11100000	100	32	10E-10	0.92
11100000	50	""	" "	0.92
11100000	5	""	" "	1.01
11100000	2	""	" "	1.04
11100000	100	24	" "	0.68
11100000	50	""	" "	0.68
11100000	5	""	" "	0.75
11100000	2	""	" "	0.98

1/2 Pupil	SNR	M	ALPHA		PIE
11100000	100	16	10E-10		1.51
11100000	50	""	"	"	2.62
11100000	5	""	"	"	2.77
11100000	2	""	"	"	2.56
11100000	100	8	"	"	0.05
11100000	50	8	"	"	0.08
11100000	5	"	"	"	1.18
11100000	2	"	"	"	1.51
00000111	100	32	"	"	1.27
00000111	100	24	"	"	1.23
00000111	100	16	"	"	2.53
00000111	100	8	"	"	1.14
11110000	100	32	"	"	0.67
11110000	50	""	"	"	0.67
11110000	5	""	"	"	0.92
11111000	2	""	"	"	1.85
11110000	100	24	"	"	0.39
11110000	50	""	"	"	0.42
11110000	5	""	"	"	0.69
11110000	2	""	"	"	2.58
11110000	100	16	"	"	0.08
11110000	50	""	"	"	0.24
11110000	5	""	"	"	0.96
11110000	2	""	"	"	1.58
11110000	100	8	"	"	0.03
11110000	50	""	"	"	0.05
11110000	5	""	"	"	0.83
11110000	2	""	"	"	0.51
11111100	100	24	"	"	0.04
11111100	100	16	"	"	0.01
11111100	100	8	"	"	0.01
11111000	100	24	"	"	0.05
11111000	100	16	"	"	0.02
11111000	100	8	"	"	0.02
11100000	100	32	0		3.28

Appendix C: Typical Data from SRES computer Program

SV = Singular Value
P*P= Autocorrelation of Pupil Vector
New Image is processed image
Error is Euclidean distance between the image and object

#	SV	P*P	OBJECT	NORMAL IMAGE	NOISY IMAGE	NEW IMAGE
1	0.320E+03	1.00	0.00	0.0072	0.1172	0.1058
2	0.256E+03	2.00	0.00	0.0200	0.0404	0.0202
3	0.256E+03	3.00	0.00	0.0120	0.0500	-0.0185
4	0.192E+03	4.00	0.00	0.0150	0.0690	0.0458
5	0.192E+03	5.00	0.00	0.0065	0.0272	-0.1081
6	0.160E+03	4.00	0.00	0.0609	0.1091	0.1246
7	0.160E+03	3.00	0.00	0.0181	0.0164	-0.0512
8	0.128E+03	2.00	0.00	0.0464	0.0515	0.1589
9	0.128E+03	1.00	0.00	0.0202	0.0330	-0.1033
10	0.128E+03	0.00	0.00	0.0244	0.0486	0.0417
11	0.128E+03	0.00	0.00	0.0318	0.0288	-0.2187
12	0.128E+03	2.00	0.00	0.4041	0.3802	0.1449
13	0.128E+03	4.00	0.00	0.2111	0.2045	0.0175
14	0.960E+02	6.00	0.00	0.5483	0.5882	0.2561
15	0.960E+02	8.00	1.00	1.0000	0.9086	0.8331
16	0.960E+02	10.00	0.00	0.3359	0.3099	-0.0431
17	0.960E+02	8.00	1.00	1.0000	1.0000	1.0000
18	0.640E+02	6.00	0.00	0.5483	0.5089	0.1799
19	0.640E+02	4.00	0.00	0.2111	0.2100	0.0013
20	0.640E+02	2.00	0.00	0.4041	0.4340	0.1429
21	0.640E+02	0.00	0.00	0.0318	0.0291	-0.1658
22	0.640E+02	0.00	0.00	0.0244	0.0334	0.0104
23	0.640E+02	1.00	0.00	0.0202	0.0198	-0.0979
24	0.320E+02	2.00	0.00	0.0464	0.0465	0.1132
25	0.320E+02	3.00	0.00	0.0181	0.0568	0.0147
26	0.320E+02	4.00	0.00	0.0609	0.0965	0.0933
27	0.320E+02	5.00	0.00	0.0065	0.0242	-0.0500
28	0.728E-04	4.00	0.00	0.0150	0.0403	-0.0031
29	0.720E-04	3.00	0.00	0.0120	0.0132	-0.0517
30	0.229E-04	2.00	0.00	0.0200	0.0184	-0.0259
31	0.205E-04	1.00	0.00	0.0072	0.1473	0.1451
32	0.146E-04	0.00	0.00	0.0399	0.0390	-0.0186

NOISY IMAGE ERROR = 1.10164
PROCESSED IMAGE ERROR = 0.62045
SNR = 5.0
ALPHA = 0.1E-09
DSEED = 3412.000

Bibliography

1. Goodman, Joseph W. Introduction to Fourier Optics. New York: McGraw-Hill Book Company, 1968.

2. Mammone, R. and G. Eichmann. "Superresolving Image Restoration Using Linear Programming," Applied Optics, 21: 496-501 (1 February 1982).

3. Harris, J.L. "Diffraction and Resolving Power," Journal of the Optical Society of America, 54: 931-936 (July 1964).

4. Frieden, B.R. "Image Enhancement and Restoration," Topics in Applied Physics, edited by T.S. Huang. New York: Springer-Verlag, 1975.

5. Hecht, Eugene and Alfred Zajac. Optics. Menlo Park, California: Addison-Wesley Publishing Company, 1979.

6. Byrne, Charles L. and others. "Image Restoration and Resolution Enhancement," Journal of the Optical Society of America, 73: 1481-1487 (November 1983).

7. Gerchberg, R.W. "Super-resolution Through Error Energy Reduction," Optica Acta, 21: 709-720 (September 1974).

8. Youla, Dante C. "Generalized Image Restoration by the Method of Alternating Orthogonal Projections," IEEE Transactions on Circuits and Systems, CAS-25: 694-702 (September 1978).

9. Cathey, W.T. and others. "Image Gathering and Processing for Enhanced Resolution," Journal of the Optical Society of America, 1: 241-250 (March 1984).

10. International Mathematical Subroutine Library

11. Golub, Gene H. and Charles F. Van Loan. Matrix Computations. Baltimore, MD.: Johns Hopkins University Press, 1983.

12. Noble, Ben and James W. Daniel. Applied Linear Algebra (2nd Ed). Englewood Cliffs, NJ: Prentice Hall Inc., 1977.

13. Gaskill, Jack D. Linear Systems, Fourier Transforms, and Optics. New York: John Wiley and Sons, 1978.

14. Rushforth, C.K. and others. "Least-squares Reconstruction of Objects with Missing High-frequency Components," Journal of the Optical Society of America, 72: 204-211 (February 1982).

15. Oppenheim Alan V. and Ronald W. Schafer. Digital Signal Processing. Englewood Cliffs, NJ: Prentice Hall Inc., 1975.

16. Jones, John. Lecture Materials distributed in MA 521, Linear Algebra. School of Engineering, Air Force Institute of Technology (AU), Wright-Patterson AFB, OH, July 1984.

17. Peebles, Peyton Z. Communications System Principles. Reading, MA: Addison-Wesley Publishing Co., 1982.

18. Etter, D.M. Structured Fortran 77 for Engineers and Scientists. Menlo Park, CA: Benjamin/Cumming Publishing Co., 1983.

VITA

Captain Robert F. Stierwalt was born on 18 December 1956 in Gadsden, Alabama. He graduated from Cass High School in Bartow County, Georgia, in 1975. He was awarded an academic scholarship to Shorter College, Rome, Georgia. He graduated from Shorter with honors with a degree in Mathematics and Chemistry. He was selected to attend Officer Training School (OTS) in June 1979. While he was at OTS, he was selected to attend the new undergraduate engineering conversion program (UECP) in residence at AFIT. He received his BSEE in March 1981. His assignment after graduating from AFIT was with the Western Space and Missile Center, 6595th Missile Test Group, Vandenberg AFB, California. He worked in the MX, later Peacekeeper, Division where he worked as a test engineer on the flight test portion of the Peacekeeper acquisition and test program. He left Vandenberg AFB in March 1984 to attend SOS enroute to the AFIT master's degree program in electrical engineering.

Permanent address: Route 3, Box 199

Gadsden, Alabama 35901

UNCLASSIFIED

SECURITY CLASSIFICATION OF THIS PAGE

REPORT DOCUMENTATION PAGE

1a. REPORT SECURITY CLASSIFICATION UNCLASSIFIED	1b. RESTRICTIVE MARKINGS
2a. SECURITY CLASSIFICATION AUTHORITY	3. DISTRIBUTION/AVAILABILITY OF REPORT Approved for public release; distribution unlimited.
2b. DECLASSIFICATION/DOWNGRADING SCHEDULE	
4. PERFORMING ORGANIZATION REPORT NUMBER(S) AFIT/GEO/ENP/85D-5	5. MONITORING ORGANIZATION REPORT NUMBER(S)
6a. NAME OF PERFORMING ORGANIZATION School of Engineering 6b. OFFICE SYMBOL (If applicable) AFIT/ENP	7a. NAME OF MONITORING ORGANIZATION
6c. ADDRESS (City, State and ZIP Code) Air Force Institute of Technology Wright-Patterson AFB, OH 45433	7b. ADDRESS (City, State and ZIP Code)
8a. NAME OF FUNDING/SPONSORING ORGANIZATION see block 19 8b. OFFICE SYMBOL (If applicable) DMLI	9. PROCUREMENT INSTRUMENT IDENTIFICATION NUMBER
8c. ADDRESS (City, State and ZIP Code) Eglin AFB, FL 32542	10. SOURCE OF FUNDING NOS. PROGRAM ELEMENT NO. | PROJECT NO. | TASK NO. | WORK UNIT NO.
11. TITLE (Include Security Classification) see block 19	

12. PERSONAL AUTHOR(S)
Robert F. Stierwalt, B.S.,B.S.E.E., Capt, USAF

13a. TYPE OF REPORT	13b. TIME COVERED	14. DATE OF REPORT (Yr., Mo., Day)	15. PAGE COUNT
MS Thesis	FROM ____ TO ____	1985 December	67

16. SUPPLEMENTARY NOTATION

17. COSATI CODES			18. SUBJECT TERMS (Continue on reverse if necessary and identify by block number)
FIELD	GROUP	SUB. GR.	Optical Filters, Incoherent Imaging Incoherent Imaging, Image Restoration
20	06		

19. ABSTRACT (Continue on reverse if necessary and identify by block number)

from block 8a. Air Force Armament Test Laboratory

Title: SUPERRESOLUTION USING INCOHERENT LIGHT AND THE LEAST SQUARES METHOD

Thesis Chairman: James P. Mills, Major, USAF
Assistant Professor of Engineering Physics

20. DISTRIBUTION/AVAILABILITY OF ABSTRACT	21. ABSTRACT SECURITY CLASSIFICATION
UNCLASSIFIED/UNLIMITED ☒ SAME AS RPT. ☐ DTIC USERS ☐	UNCLASSIFIED

22a. NAME OF RESPONSIBLE INDIVIDUAL	22b. TELEPHONE NUMBER (Include Area Code)	22c. OFFICE SYMBOL
James P. Mills, Major, USAF	513-255-2012	AFIT/ENP

This thesis discusses the problem of incoherent imaging in a diffraction-limited optical system. The purpose of the thesis was to prove that resolving two incoherent point sources of light is possible and achievable under certain circumstances. The effects of noise are considered when trying to superresolve the two incoherent objects.

The analysis assumes a finite object of known maximum extent with an estimation of the noise in the system. The noise is assumed to be Gaussian, white, and additive for all spatial frequencies. The superresolution process uses the standard least squares process to achieve minimum error with a smoothing or regularization procedure. The singular values of the transfer matrix are modified to attenuate the very small singular values to avoid noise amplification in the high order terms. The effect of the noise is overcome by the use of a smoothing parameter, α, as shown in the results. The superresolution process works extremely well when the extent of the object is known a priori to have a certain bound or maximum. Components of the restored or processed object outside the known bounds are attenuated. The results indicate that band-pass pupils can superresolve with only limited knowledge of the object when the smoothing parameter is used.